

O. Babelon, B. Douçot

Laboratoire de Physique Théorique et Hautes Energies¹, (LPTHE)
 Unité Mixte de Recherche UMR 7589
 Université Pierre et Marie Curie-Paris 6 and CNRS;

Abstract: The Jaynes-Cummings-Gaudin model describes a collection of n spins coupled to an harmonic oscillator. It is known to be integrable, so one can define a moment map which associates to each point in phase-space the list of values of the $n + 1$ conserved Hamiltonians. We identify all the critical points of this map and we compute the corresponding quadratic normal forms, using the Lax matrix representation of the model. The normal coordinates are constructed by a procedure which appears as a classical version of the Bethe Ansatz used to solve the quantum model. We show that only elliptic or focus-focus singularities are present in this model, which provides an interesting example of a symplectic toric action with singularities. To explore these, we study in detail the degeneracies of the spectral curves for the $n = 1$ and $n = 2$ cases. This gives a complete picture for the image of the momentum map (IMM) and the associated bifurcation diagram. For $n = 2$ we found in particular some lines of rank 1 which lie, for one part, on the boundary of the IMM, where they behave like an edge separating two faces, and which go, for another part, inside the IMM.

1 Introduction.

Suppose we have a Hamiltonian system with Hamiltonian H on a phase space of dimension $2n$ with coordinates x_1, \dots, x_{2n} . A critical point $x_j^{(0)}$ is an equilibrium point

$$\left. \frac{\partial H}{\partial x_j} \right|_{x_j=x_j^{(0)}} = 0, \quad j = 1, \dots, 2n$$

We can expand the Hamiltonian around such a point, $x_j = x_j^{(0)} + \delta x_j$, getting a quadratic form

$$H = H^{(0)} + Q + \dots, \quad Q = \sum_{i,j} Q_{ij} \delta x_i \delta x_j$$

The question then arises to simplify or “diagonalize” the quadratic form Q . This problem is simple if we allow $Sl_{2n}(R)$ transformations of the δx_j , the matrix Q_{ij} can then be diagonalized in the orthogonal group. However in the present case the natural group is the group of symplectic

¹Tour 13-14, 4ème étage, Boite 126, 4 Place Jussieu, 75252 Paris Cedex 05.

transformations and the diagonalization problem is not straightforward. Its solution has been given by Williamson [1, 2] in terms of six families of elementary quadratic forms on which we can decompose H . Each family corresponds to a certain pattern of eigenvalues of the associated linear Hamiltonian flow. There are two families for the eigenvalue 0, a third one for a pair of opposite real eigenvalues (hyperbolic flow), two more for a pair of purely imaginary eigenvalues (elliptic flow), and the last one for quartets of complex eigenvalues of the form $\pm\alpha \pm i\beta$. Besides diagonal blocks, each family admits non-diagonal Jordan blocks of unlimited size.

The above problem of reducing H to its normal form is not completely trivial. Even less trivial is the case of an integrable system, in which case we have n Poisson commuting Hamiltonians H_i . These functions define the moment map, from R^{2n} to R^n , which sends x to $(H_1(x), \dots, H_n(x))$. A critical point is a simultaneous critical point for all the H_i , in other words, it is a point at which the differential of the moment map vanishes. Expanding the H_i around such a point, we get n Poisson commuting quadratic forms Q_i . For each of them, Williamson theorem applies, but since they commute, we can reduce them to normal forms simultaneously. The simplest case is of a nondegenerate singularity, for which the Hamiltonian flows associated to the n quadratic forms Q_i realize a Cartan subalgebra of the Lie algebra $sp_n(R)$. The fact that each Q_i Poisson commutes with the others yields strong constraints on the form of the elementary blocks which can appear in the Williamson reduction of Q_i . It turns out that integrability excludes non-diagonal Jordan blocks, therefore there exist canonical coordinates $q_1, \dots, q_n, p_1, \dots, p_n$ such that the above quadratic forms can be reduced into the following quadratic polynomials: [3]

$$\begin{aligned} P_j^{\text{elliptic}} &= p_j^2 + q_j^2, \quad j = 1, 2, \dots, m_1 \\ P_j^{\text{hyperbolic}} &= p_j q_j, \quad j = m_1 + 1, \dots, m_1 + m_2 \\ P_j^{\text{focus-focus}} &= p_j q_j + p_{j+1} q_{j+1}, \quad j = m_1 + m_2 + 1 \dots \\ P_{j+1}^{\text{focus-focus}} &= p_j q_{j+1} - p_{j+1} q_j, \quad \dots, m_1 + m_2 + 2m_3 \end{aligned}$$

where $m_1 + m_2 + 2m_3 = n$. The triple (m_1, m_2, m_3) is called the type of the critical point. It encodes all the qualitative information on the system, in particular on the dimensions of fibers of the moment map in the vicinity of the corresponding critical value. The above set of quadratic forms is referred to as the normal form for a non-degenerate critical point of an integrable system.

In the focus-focus case, $P_j^{\text{focus-focus}}$ and $P_{j+1}^{\text{focus-focus}}$ can be combined into a single complex quantity. Setting

$$B_j = p_j + ip_{j+1}, \quad B_{j+1} = q_j + iq_{j+1}$$

we have

$$B_j \bar{B}_{j+1} = P_j^{\text{focus-focus}} - iP_{j+1}^{\text{focus-focus}}$$

In this paper we observe that the solution to this problem of the simultaneous reduction of the conserved Hamiltonians in the vicinity of critical points is the classical analog of Bethe Ansatz which is used to diagonalize simultaneously the *quantum* commuting Hamiltonians H_i . We demonstrate it

on the particular example of the Jaynes-Cummings-Gaudin model [4, 5, 6, 7], but the construction is clearly a general one. As a result we will show that, in this model, singularities are only of two types: elliptic and focus-focus.

The above critical points are the points where the moment map

$$R^{2n} \rightarrow R^n : \quad x \rightarrow (H_1(x), \dots, H_n(x))$$

is of rank zero. Other manifolds where the rank of the moment map is not maximal are also of great interest. Their images in R^n by the moment map constitute the bifurcation diagram. As explained in particular by Michèle Audin [8], a powerful tool to construct this diagram for an integrable model is the correspondence between singularities of the moment map and degeneracies of the associated spectral curve. We will show explicitly the results of this method for the Jaynes-Cummings-Gaudin model with two and three degrees of freedom.

Another advantage of this model is that it admits one free parameter for each degree of freedom. The types of the critical points therefore depend on these parameters. In particular, it is possible to choose them in such a way that all the critical points are of the elliptic type. In this case, the Hamiltonian flows of the conserved H_i can be used to define a torus action on phase space. A famous theorem states that, if we replace the H_i 's by the corresponding action variables, the image of the moment map is a convex polytope [9, 10]. However, for most values of the parameters, focus-focus singularities appear which provides examples of the more general “almost toric” action studied in [11], and the important phenomenon of “monodromy” discovered in [12], preventing the existence of global action-angle variables, comes into play.

While the one-spin Jaynes-Cummings model was already re-discovered by mathematicians [13], it seems that the results concerning the bifurcation diagrams of the two-spin Jaynes-Cummings model are new. The geometric richness of these diagrams undoubtedly calls for further studies.

The paper is organized as follows. In section 2 we present the Jaynes-Cummings-Gaudin model and recall some basic facts about its Lax representation. In section 3 we study the critical points of the model and their normal forms are computed in section 4 using a classical analog of Bethe Ansatz. In section 5 we discuss the monodromy. Section 6 is a short introduction to separated variables and explains that the different strata of the bifurcation diagram correspond to the degeneracies of the spectral curve. In sections 7 and 8 we study the bifurcation diagram for the one-spin and two-spin models respectively.

2 The classical Jaynes-Cummings-Gaudin model.

This model, where a collection of n spins is coupled to a single harmonic oscillator, has been used for more than fifty years in atomic physics to describe the interaction of an ensemble of atoms with a mode of the quantized electromagnetic field [4, 5, 6, 7, 14]. It derives from the following

Hamiltonian:

$$H = \sum_{j=1}^n (2\epsilon_j + \omega) s_j^z + \omega \bar{b} b + \sum_{j=1}^n (\bar{b} s_j^- + b s_j^+) \quad (1)$$

The \vec{s}_j are spin variables, and b, \bar{b} is a harmonic oscillator. The Poisson brackets read

$$\{s_j^a, s_j^b\} = -\epsilon_{abc} s_j^c, \quad \{b, \bar{b}\} = i \quad (2)$$

The \vec{s}_j brackets are degenerate. We fix the value of the Casimir functions

$$\vec{s}_j \cdot \vec{s}_j = s^2$$

Phase space has dimension $2(n+1)$. In the Hamiltonian we have used

$$s_j^\pm = s_j^1 \pm i s_j^2$$

which have Poisson brackets

$$\{s_j^z, s_j^\pm\} = \pm i s_j^\pm, \quad \{s_j^+, s_j^-\} = 2i s_j^z$$

The equations of motion read

$$\dot{b} = -i \frac{\partial H}{\partial \bar{b}} = -i \omega b - i \sum_{j=1}^n s_j^- \quad (3)$$

$$\dot{s}_j^z = -i \frac{\partial H}{\partial s_j^+} s_j^+ + i \frac{\partial H}{\partial s_j^-} s_j^- = i(\bar{b} s_j^- - b s_j^+) \quad (4)$$

$$\dot{s}_j^+ = i \frac{\partial H}{\partial s_j^z} s_j^+ - 2i \frac{\partial H}{\partial s_j^-} s_j^z = i(2\epsilon_j + \omega) s_j^+ - 2i \bar{b} s_j^z \quad (5)$$

$$\dot{s}_j^- = -i \frac{\partial H}{\partial s_j^z} s_j^- + 2i \frac{\partial H}{\partial s_j^+} s_j^z = -i(2\epsilon_j + \omega) s_j^- + 2i b s_j^z \quad (6)$$

This is an integrable system. To see it we introduce the Lax matrices

$$L(\lambda) = 2\lambda \sigma^z + 2(b\sigma^+ + \bar{b}\sigma^-) + \sum_{j=1}^n \frac{\vec{s}_j \cdot \vec{\sigma}}{\lambda - \epsilon_j} \quad (7)$$

$$M(\lambda) = -i\lambda \sigma^z - i\frac{\omega}{2} \sigma^z - i(b\sigma^+ + \bar{b}\sigma^-) \quad (8)$$

where σ^a are the Pauli matrices.

$$\sigma^x = \begin{pmatrix} 0 & 1 \\ 1 & 0 \end{pmatrix}, \quad \sigma^y = \begin{pmatrix} 0 & -i \\ i & 0 \end{pmatrix}, \quad \sigma^z = \begin{pmatrix} 1 & 0 \\ 0 & -1 \end{pmatrix},$$

and we have defined

$$\sigma^\pm = \frac{1}{2}(\sigma^x \pm i\sigma^y), \quad [\sigma^z, \sigma^\pm] = \pm 2\sigma^\pm, \quad [\sigma^+, \sigma^-] = \sigma^z$$

It is not difficult to check that the equations of motion are equivalent to the Lax equation

$$\dot{L}(\lambda) = [M(\lambda), L(\lambda)] \quad (9)$$

Let

$$L(\lambda) = \begin{pmatrix} A(\lambda) & B(\lambda) \\ C(\lambda) & -A(\lambda) \end{pmatrix}$$

we have

$$A(\lambda) = 2\lambda + \sum_{j=1}^n \frac{s_j^z}{\lambda - \epsilon_j} \quad (10)$$

$$B(\lambda) = 2b + \sum_{j=1}^n \frac{s_j^-}{\lambda - \epsilon_j} \quad (11)$$

$$C(\lambda) = 2\bar{b} + \sum_{j=1}^n \frac{s_j^+}{\lambda - \epsilon_j} \quad (12)$$

One has the simple Poisson brackets

$$\{A(\lambda), A(\mu)\} = 0 \quad (13)$$

$$\{B(\lambda), B(\mu)\} = 0 \quad (14)$$

$$\{C(\lambda), C(\mu)\} = 0 \quad (15)$$

$$\{A(\lambda), B(\mu)\} = \frac{i}{\lambda - \mu}(B(\lambda) - B(\mu)) \quad (16)$$

$$\{A(\lambda), C(\mu)\} = -\frac{i}{\lambda - \mu}(C(\lambda) - C(\mu)) \quad (17)$$

$$\{B(\lambda), C(\mu)\} = \frac{2i}{\lambda - \mu}(A(\lambda) - A(\mu)) \quad (18)$$

One can rewrite these equations in the usual classical r -matrix form

$$\{L_1(\lambda), L_2(\mu)\} = -i \left[\frac{P_{12}}{\lambda - \mu}, L_1(\lambda) + L_2(\mu) \right]$$

where

$$P_{12} = \begin{pmatrix} 1 & 0 & 0 & 0 \\ 0 & 0 & 1 & 0 \\ 0 & 1 & 0 & 0 \\ 0 & 0 & 0 & 1 \end{pmatrix}$$

It follows immediately that $\text{Tr}(L^2(\lambda)) = 2A^2(\lambda) + 2B(\lambda)C(\lambda)$ Poisson commute for different values of the spectral parameter:

$$\{\text{Tr}(L^2(\lambda_1)), \text{Tr}(L^2(\lambda_2))\} = 0$$

Hence $\Lambda(\lambda) \equiv \frac{1}{2}\text{Tr}(L^2(\lambda))$ generates Poisson commuting quantities. One has

$$\Lambda(\lambda) = \frac{Q_{2n+2}(\lambda)}{\prod_j(\lambda - \epsilon_j)^2} = 4\lambda^2 + 4H_{n+1} + 2\sum_{j=1}^n \frac{H_j}{\lambda - \epsilon_j} + \sum_{j=1}^n \frac{s^2}{(\lambda - \epsilon_j)^2} \quad (19)$$

where the $(n+1)$ Hamiltonians H_j , $j = 1, \dots, n+1$ read

$$H_{n+1} = b\bar{b} + \sum_j s_j^z \quad (20)$$

and

$$H_j = 2\epsilon_j s_j^z + (bs_j^+ + \bar{b}s_j^-) + \sum_{k \neq j} \frac{s_j \cdot s_k}{\epsilon_j - \epsilon_k}, \quad j = 1, \dots, n \quad (21)$$

One can easily verify that, indeed, $\{H_i, H_j\} = 0$ for $i, j = 1, \dots, n+1$, hence the system is integrable. The Hamiltonian eq.(1) is

$$H = \omega H_{n+1} + \sum_{j=1}^n H_j$$

3 Critical points

The critical points are equilibrium points for all the Hamiltonians H_j , $j = 1, \dots, n+1$. At such points the derivatives with respect of all coordinates on phase space vanish. In particular, since

$$\frac{\partial H_{n+1}}{\partial \bar{b}} = b, \quad \frac{\partial H_j}{\partial \bar{b}} = s_j^-$$

we see that the critical points must be located at

$$b = \bar{b} = 0, \quad s_j^\pm = 0, \quad s_j^z = e_j s, \quad e_j = \pm 1 \quad (22)$$

When we expand around a configuration eq.(22), all the quantities $(b, \bar{b}, s_j^+, s_j^-)$ are first order, but s_j^z is second order because

$$s_j^z = e_j \sqrt{s^2 - s_j^+ s_j^-} = se_j - \frac{e_j}{2s} s_j^+ s_j^- + \dots, \quad e_j = \pm 1$$

It is then simple to see that all first order terms in the expansions of the Hamiltonians H_j vanish. Hence we have found 2^n critical points.

4 Normal Forms.

We want to expand the Hamiltonians H_j around the equilibrium points eq.(22) and write them in normal form. Symbolically :

$$H_j = \sum_{\alpha} E_{j,\alpha} \bar{a}_{\alpha} a_{\alpha} \quad (23)$$

where $\bar{a}_{\alpha}, a_{\alpha}$ are independent harmonic oscillators (in the elliptic case). Note that if we quantize the above Hamiltonians in this approximation, their diagonalization is immediate: the normal coordinates a_{α} become spectrum generating operators. Their construction must therefore be very much related to the simultaneous diagonalization of the H_j . But the tool to solve this problem is well known: Bethe Ansatz.

Inspired by this remark, we return to eqs.(10 – 12) and eqs.(13 – 18). Now, we have

$$\left\{ \frac{1}{2} \text{Tr} L^2(\lambda), C(\mu) \right\} = \frac{2i}{\lambda - \mu} \left(A(\lambda)C(\mu) - A(\mu)C(\lambda) \right)$$

When we expand around a critical point, the Hamiltonians are quadratic. Remark that $C(\mu)$ is first order and therefore the Poisson bracket in left hand side is linear. Now $A(\lambda)$ is constant plus second order, so that in the right-hand side we can replace $A(\lambda)$ and $A(\mu)$ by their zeroth order expression :

$$A(\lambda) \simeq a(\lambda) = 2\lambda + \sum_{j=1}^n \frac{se_j}{\lambda - \epsilon_j}$$

and we arrive at

$$\left\{ \frac{1}{2} \text{Tr} L^2(\lambda), C(\mu) \right\} = \frac{2i}{\lambda - \mu} \left(a(\lambda)C(\mu) - a(\mu)C(\lambda) \right) \quad (24)$$

Going back to eq.(23), we see that the a_{α} are such that

$$\{H_j, a_{\alpha}\} = E_{j,\alpha} a_{\alpha} \quad (25)$$

Eq.(24) will be precisely of the form of eq.(25) if we can kill the unwanted term $C(\lambda)$. This is achieved by imposing the condition

$$a(\mu) = 0, \quad \text{“Classical Bethe Equation”} \quad (26)$$

This is an equation of degree $n + 1$ for μ . Calling μ_i its solutions, we construct in this way $n + 1$ variables $C(\mu_i)$. Remark that by eq.(15), they all commute

$$\{C(\mu_i), C(\mu_j)\} = 0 \quad (27)$$

Since phase space has dimension $2(n+1)$ this is half what we need. To construct the conjugate variables, we consider eq.(18). In our linear approximation it reads

$$\{B(\mu_i), C(\mu_j)\} = \frac{2i}{\mu_i - \mu_j} (a(\mu_i) - a(\mu_j))$$

If μ_i and μ_j are *different* solutions of eq.(26), then obviously

$$\{B(\mu_i), C(\mu_j)\} = 0, \quad \mu_i \neq \mu_j \quad (28)$$

If however $\mu_j = \mu_i$ then

$$\{B(\mu_i), C(\mu_i)\} = 2ia'(\mu_i) \quad (29)$$

Finally, by eq.(14) we have

$$\{B(\mu_i), B(\mu_j)\} = 0 \quad (30)$$

Up to normalisation, we have indeed constructed canonical coordinates !

It is simple to express the quadratic Hamiltonians in these coordinates:

$$\frac{1}{2} \text{Tr} L^2(\lambda) = a^2(\lambda) + \sum_j \frac{a(\lambda)}{a'(\mu_j)(\lambda - \mu_j)} B(\mu_j) C(\mu_j) \quad (31)$$

This has the correct analytical properties in λ and together with the Poisson brackets eqs.(27,28, 29, 30) we reproduce eq.(24). Note that there is no pole at $\lambda = \mu_j$ because $a(\mu_j) = 0$. Expanding around $\lambda = \infty$ we get

$$H_{n+1} = s \sum_k e_k + \sum_i \frac{1}{2a'(\mu_i)} B(\mu_i) C(\mu_i)$$

and computing the residue at $\lambda = \epsilon_j$, we find

$$H_j = se_j \left[2\epsilon_j + \sum_k \frac{se_k}{\epsilon_j - \epsilon_k} \right] + \sum_i \frac{1}{2a'(\mu_i)} \frac{se_j}{\epsilon_j - \mu_i} B(\mu_i) C(\mu_i)$$

We can invert these formulae: divide eq.(31) by $\lambda - \mu_j$ and take the residue at $\lambda = \mu_j$. Since $a(\mu_j) = 0$ we get

$$\frac{1}{2} \text{Tr} L^2(\mu_j) = B(\mu_j) C(\mu_j)$$

or explicitly

$$B(\mu_j) C(\mu_j) = 4\mu_j^2 + 4H_{n+1} + \sum_{k=1}^n \frac{2H_k}{\mu_j - \epsilon_k} + \sum_{k=1}^n \frac{s^2}{(\mu_j - \epsilon_k)^2}$$

We can now make contact with the Williamson classification theorem.

If μ_j is *real* we have $B(\mu_j) = \overline{C(\mu_j)}$ and we set

$$C(\mu_j) = \sqrt{|a'(\mu_j)|}(p_j + i\epsilon_j q_j), \quad B(\mu_j) = \sqrt{|a'(\mu_j)|}(p_j - i\epsilon_j q_j)$$

where $\epsilon_j = -\text{sign}(a'(\mu_j))$ and p_j, q_j are canonical coordinates. Then eq.(29) is satisfied. Moreover

$$B(\mu_j)C(\mu_j) = |a'(\mu_j)|(p_j^2 + q_j^2)$$

i.e. we have an *elliptic* singularity.

If μ_j is *complex*, there is another root $\mu_{j+1} = \bar{\mu}_j$ which is its complex conjugate. Then $\overline{B(\mu_j)} = C(\mu_{j+1})$. We introduce canonical coordinates $p_j, q_j, p_{j+1}, q_{j+1}$ and set

$$B(\mu_j) = -ia'(\mu_j)(q_j + iq_{j+1}), \quad B(\mu_{j+1}) = p_j + ip_{j+1}$$

$$C(\mu_j) = p_j - ip_{j+1}, \quad C(\mu_{j+1}) = ia'(\mu_{j+1})(q_j - iq_{j+1})$$

then eqs.(27,28,29,30) are satisfied and

$$\begin{aligned} B(\mu_j)C(\mu_j) &= -ia'(\mu_j)(P_j^{\text{focus-focus}} + iP_{j+1}^{\text{focus-focus}}) \\ B(\mu_{j+1})C(\mu_{j+1}) &= ia'(\mu_{j+1})(P_j^{\text{focus-focus}} - iP_{j+1}^{\text{focus-focus}}) \end{aligned}$$

i.e. we have a *focus-focus* singularity.

It remains to see when the classical Bethe roots are real and when they are complex. Let us assume all the spins are down: $e_j = -1, j = 0, \dots, n-1$. The condition $a(\mu) = 0$ reads

$$\mu = \frac{s}{2} \sum_i \frac{1}{\mu - \epsilon_i} \quad (32)$$

The graph of the curves $y = \mu$ and $y = \frac{s}{2} \sum_{j=1}^n \frac{1}{\mu - \epsilon_j}$ are presented in Fig.[1]. In that case we have $n+1$ *real* roots. The singularity is elliptic meaning that this critical point is locally stable. This is the situation that prevails when $\sum e_i < 0$.

Suppose now that $e_j = 1, j = 0, \dots, n-1$. The graph of the curves $y = \mu$ and $y = -\frac{s}{2} \sum_{j=1}^n \frac{1}{\mu - \epsilon_j}$ are presented in Fig [2]. The situation is more complex, we can have $n-1$ real roots and a *pair of complex conjugated roots*, or $n+1$ real roots, depending on the values of the ϵ_j .

This situation prevails when $\sum e_i > 0$. When $\sum e_i = 0$, the driving parameter is $\sum \epsilon_i e_i$.

Normal forms can be used to compute the dimension of the preimage of a singular point. Fixing the values of the conserved quantities amount to fix the values of the quadratic terms. For an elliptic term we have

$$p_j^2 + q_j^2 = h_j$$

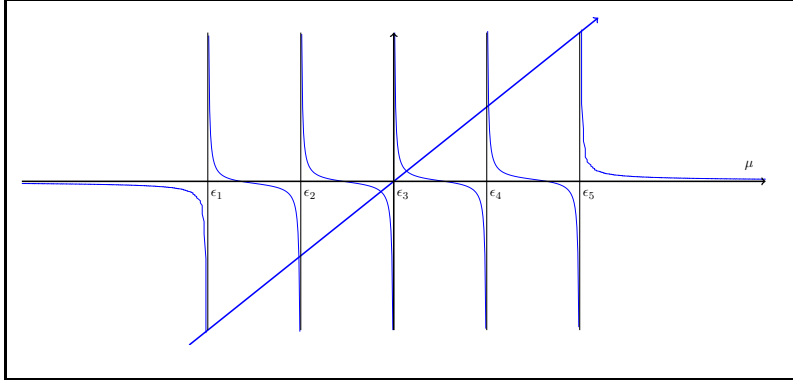


Figure 1: The solutions of eq.(32) when $e_j = -1$.

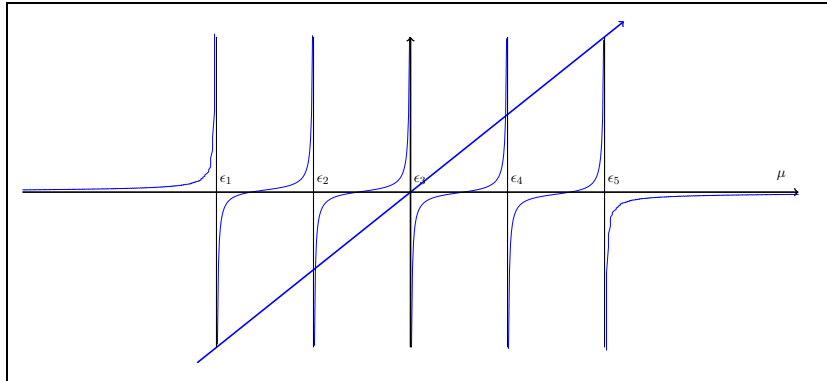


Figure 2: The solutions of eq.(32) when $e_j = 1$.

and the preimage is a circle. If $h_j = 0$ this circle degenerates to a point. In the case of a focus-focus singularity we have

$$\begin{aligned} p_j q_j + p_{j+1} q_{j+1} &= h_j \\ p_j q_{j+1} - p_{j+1} q_j &= h_{j+1} \end{aligned}$$

Solving in p_i for instance we find

$$p_j = \frac{h_j q_j + h_{j+1} q_{j+1}}{q_j^2 + q_{j+1}^2}, \quad p_{j+1} = \frac{h_j q_{j+1} - h_{j+1} q_j}{q_j^2 + q_{j+1}^2}$$

so we have a two dimensional preimage. If $h_j = h_{j+1} = 0$, we have two planes $q_j = q_{j+1} = 0$ or $p_j = p_{j+1} = 0$ which intersect in one point. The preimage is a pinched torus.

5 Monodromy.

Let us go back to eq.(31). We have

$$\frac{Q_{2n+2}(\lambda)}{\prod_j (\lambda - \epsilon_j)^2} = a^2(\lambda) + \sum_j \frac{a(\lambda)}{a'(\mu_j)(\lambda - \mu_j)} B(\mu_j) C(\mu_j) \quad (33)$$

Of course

$$a(\lambda) = 2 \frac{\prod_j (\lambda - \mu_j)}{\prod_j (\lambda - \epsilon_j)}$$

We want to study the roots of the polynomial $Q_{2n+2}(\lambda)$ when we perform a small circle around the singularity in the space H_i i.e. we want to examine the motion of the branch points of the spectral curve (to be defined in the next section, see eq. (34)) when we turn around a singularity. To zeroth order in the small deviations b, \bar{b}, s_j^\pm away from a critical point, the polynomials $B(\lambda)$ and $C(\lambda)$ vanish, whereas $A(\lambda)$ can be replaced by the fixed function $a(\lambda)$. Therefore:

$$\frac{Q_{2n+2}(\lambda)}{\prod_j (\lambda - \epsilon_j)^2} = a^2(\lambda)$$

and $Q_{2n+2}(\lambda)$ has double zeroes at the roots μ_j of the classical Bethe equation $a(\mu_j) = 0$. Let us now pick a phase-space point close to the critical point. The corresponding invariant polynomial $Q_{2n+2}(\lambda)$ is expressed in terms of the normal coordinates $B(\mu_j), C(\mu_j)$ through eq.(33) Consider a root μ_j . The branch point is moved at $\mu_j + \delta\mu_j$. Inserting into eq.(33) we get the equation

$$(\delta\mu_j)^2 = - \left(\frac{1}{a'(\mu_j)} \right)^2 B(\mu_j) C(\mu_j)$$

so the leading variation of the root μ_j is due to the normal mode $B(\mu_j), C(\mu_j)$ only. The other modes contribute in subdominant terms. This is Krichever's result [15].

If the root μ_j is real, we see that that it splits into a pair of complex conjugated roots, and the splitting is in the imaginary direction. To first order the deformation space is one dimensional, because, as we have seen, $B(\mu_j) = \overline{C(\mu_j)}$.

If the root μ_j is complex then $(\delta\mu_j)^2$ is complex.

$$(\delta\mu_j)^2 = - \left(\frac{1}{a'(\mu_j)} \right)^2 B(\mu_j)C(\mu_j) = \frac{i}{a'(\mu_j)} (P_j^{focus-focus} + iP_{j+1}^{focus-focus})$$

The deformation space to leading order is now two dimensional. When we perform a small loop around the singularity in H -space, the branch points perform half a turn in opposite directions and at the end of the process they are exchanged. This is the basis of the interpretation by Michèle Audin [16] of the monodromy [12, 17, 18, 20] using Picard-Lefschetz theory.

6 Riemann surfaces and integrability.

In this section we recall, in the example of the Jaynes-Cummings-Gaudin model, the algebro-geometric solution of classical integrable models [21, 22, 23, 24]. We first introduce the spectral curve. At each point of the spectral curve we can associate an eigenvector of the Lax matrix. When properly normalised the components of this eigenvector are meromorphic functions on the spectral curve. The poles of these meromorphic functions are coordinates on phase space. We compute their Poisson brackets. The image of the divisor of the poles by the Abel map is a point on the Jacobian. The motion of this point under the Hamiltonians of the system is linear. We deduce from this that when the spectral curve is non degenerate, the image of the moment map has maximal rank.

The spectral curve is a curve in \mathbb{C}^2 defined as $\det(L(\lambda) - \mu) = 0$ or:

$$\Gamma : \mu^2 - A^2(\lambda) - B(\lambda)C(\lambda) = 0 \tag{34}$$

Its importance arises from the fact that it is invariant under the time evolution, so it encodes knowledge of all the commuting integrals of motion. Equivalently, a spectral curve is attached to each fiber of the moment map. In the Jaynes-Cummings-Gaudin model, its equation reads:

$$\mu^2 = 4\lambda^2 + 4H_{n+1} + 2 \sum_{j=1}^n \frac{H_j}{\lambda - \epsilon_j} + \sum_{j=1}^n \frac{s^2}{(\lambda - \epsilon_j)^2}$$

We will consider the system reduced by the symmetry generated by H_{n+1} . It acts on the Lax matrix by conjugation by a diagonal matrix and obviously leaves the spectral curve invariant. Hence the dynamical Hamiltonians are H_j , $j = 1, \dots, n$, and H_{n+1} should be considered as a

constant parameter. Note that the dynamical Hamiltonians H_j appear linearly in the equation of the spectral curve:

$$\Gamma : R(\lambda, \mu) \equiv R_0(\lambda, \mu) + \sum_{j=1}^g R_j(\lambda) H_j = 0 \quad (35)$$

where:

$$R_j(\lambda) = \frac{2}{\lambda - \epsilon_j}, \quad R_0(\lambda, \mu) = -\mu^2 + 4\lambda^2 + 4H_{n+1} + \sum_j \frac{s^2}{(\lambda - \epsilon_j)^2}$$

As we already noticed

$$A^2(\lambda) + B(\lambda)C(\lambda) = \frac{Q_{2n+2}(\lambda)}{\prod_j (\lambda - \epsilon_j)^2}$$

where $Q_{2n+2}(\lambda)$ is a polynomial of degree $2n + 2$. Defining $y = \mu \prod_j (\lambda - \epsilon_j)$, the equation of the spectral curve becomes

$$y^2 = Q_{2n+2}(\lambda)$$

which is an hyperelliptic curve of genus $g = n$. The dimension of the phase space of the model is $2(n + 1)$. However, we reduced it by the action of the group of conjugation by diagonal matrices which is of dimension 1. Hence we confirm that

$$g = \frac{1}{2} \dim \mathcal{M}_{\text{reduced}} = n$$

At each point of the spectral curve, we can solve the equation

$$(L(\lambda) - \mu) \Psi = 0$$

Normalizing the second component (instead of the first one, for later convenience) of Ψ to be 1, we find:

$$\Psi = \begin{pmatrix} \psi_1 \\ 1 \end{pmatrix}, \quad \psi_1 = \frac{A(\lambda) + \mu}{C(\lambda)}$$

showing that ψ_1 is a meromorphic functions on the spectral curve. The poles of Ψ at finite distance are located above the zeroes of $C(\lambda)$. Note that if $C(\lambda_k) = 0$, then the points on Γ above λ_k have coordinates $\mu_k = \pm A(\lambda_k)$. The pole of Ψ is at the point $\mu_k = A(\lambda_k)$, since at the other point, $\mu_k = -A(\lambda_k)$, the numerator of ψ_1 has a zero.

Recalling that

$$C(\lambda) = 2\bar{b} + \sum_{j=1}^n \frac{s_j^+}{\lambda - \epsilon_j} \equiv 2\bar{b} \frac{\prod_{k=1}^n (\lambda - \lambda_k)}{\prod_{j=1}^n (\lambda - \epsilon_j)} \quad (36)$$

we see that indeed the eigenvector has $n = g$ dynamical poles.

At infinity, we have two points:

$$Q_{\pm} : \mu = \pm 2\lambda(1 + O(\lambda^{-2}))$$

Remembering that

$$A(\lambda) = 2\lambda + O(\lambda^{-1}), \quad C(\lambda) = 2\bar{b} + O(\lambda^{-1})$$

we find the following behavior of the function ψ_1 at the two points Q_{\pm}

$$Q_+ : \psi_1 = \frac{2}{\bar{b}} \lambda + O(\lambda^{-1}), \quad Q_- : \psi_1 = O(\lambda^{-1})$$

showing that the eigenvector has a pole at Q_+ and a zero at Q_- in agreement with the general theory. By the Riemann-Roch theorem, the meromorphic function ψ_1 exists and is unique.

We can reconstruct the phase-space point of the reduced model (where H_{n+1} is a fixed parameter) from the knowledge of the $2n$ variables (λ_k, μ_k) . From eq. (36), we get:

$$s_j^+ = 2\bar{b} \frac{\prod_{k=1}^n (\epsilon_j - \lambda_k)}{\prod_{i \neq j} (\epsilon_j - \epsilon_i)} \quad (37)$$

The s_j^z components can be obtained from the n equations:

$$\mu_k - 2\lambda_k = \sum_{j=1}^n \frac{s_j^z}{\mu_k - \epsilon_j}$$

after inversion of a Cauchy matrix. This analysis shows that the Lax matrix can be reconstructed once we know the coordinates (λ_k, μ_k) of the poles of the eigenvectors. Hence (λ_k, μ_k) can be considered as coordinates on the (reduced) phase space. We now compute the symplectic form in these coordinates.

From the constraint $(s_j^z)^2 + s_j^+ s_j^- = s^2$ we can eliminate the variables s_j^- . Remembering the Poisson bracket $\{s_j^z, s_j^+\} = i s_j^+$, we can write the symplectic form as

$$\Omega = -i\delta b \wedge \delta \bar{b} + i \sum_j \frac{\delta s_j^+}{s_j^+} \wedge \delta s_j^z$$

From eq.(37), we get:

$$\frac{\delta s_j^+}{s_j^+} = \frac{\delta \bar{b}}{\bar{b}} + \sum_k \frac{\delta \lambda_k}{\lambda_k - \epsilon_j}$$

therefore:

$$\Omega = -i\delta b \wedge \delta \bar{b} + i \frac{\delta \bar{b}}{\bar{b}} \wedge \sum_j \delta s_j^z + i \sum_k \sum_j \frac{\delta \lambda_k \wedge \delta s_j^z}{\lambda_k - \epsilon_j}$$

But

$$\delta A(\lambda_k) = 2\delta\lambda_k + \sum_j \frac{\delta s_j^z}{\lambda_k - \epsilon_j} - \frac{s_j^z}{(\lambda_k - \epsilon_j)^2} \delta\lambda_k$$

and

$$\Omega = i \frac{\delta \bar{b}}{\bar{b}} \wedge \left[\delta(b\bar{b}) + \sum_j \delta s_j^z \right] + i \sum_k \delta\lambda_k \wedge \delta A(\lambda_k)$$

Finally:

$$\Omega = i \delta \log \bar{b} \wedge \delta H_{n+1} + i \sum_k \delta\lambda_k \wedge \delta\mu_k$$

This shows that the variables (λ_k, μ_k) are canonically conjugate. The above calculation is valid before the symplectic reduction by H_{n+1} . This expression for the symplectic form confirms that the separated variables are invariant under the diagonal group action

$$\{H_{n+1}, \lambda_k\} = 0, \quad \{H_{n+1}, \mu_k\} = 0 \quad (38)$$

so that they can be used as coordinates on the reduced phase space.

We have found that Γ is of genus $g = n$ and there are exactly g commuting Hamiltonians H_j . Moreover Ψ has exactly g dynamical poles. The curve is completely determined by requiring that it passes through the g points (λ_i, μ_i) , $i = 1, \dots, g$. Indeed, the Hamiltonians H_j are determined by solving the linear system

$$\sum_j \frac{1}{\lambda_k - \epsilon_j} H_j = \frac{1}{2} \mu_k^2 - 2\lambda_k^2 - 2H_{n+1} - \frac{1}{2} \sum_j \frac{s^2}{(\lambda_k - \epsilon_j)^2} \quad (39)$$

whose solution is

$$H = B^{-1}V \quad (40)$$

Here the matrix B_{kj} is the Cauchy matrix

$$B_{kj} = \frac{1}{\lambda_k - \epsilon_j} \quad (41)$$

and V_k is the right hand side of eq.(39).

We now compute the equations of motion of the λ_k 's. One has

$$\partial_{t_i} \lambda_k = \{H_i, \lambda_k\} = - \sum_l \{B_{il}^{-1} V_l, \lambda_k\} = - \sum_l B_{il}^{-1} \{V_l, \lambda_k\} = -B_{ik}^{-1} \{V_k, \lambda_k\}$$

where in the last equality, we used the separated structure of the matrix B and the vector V to suppress the sum over l . Explicitly

$$\partial_{t_i} \lambda_k = -i(B^{-1})_{ik} \mu_k \quad (\text{no summation over } k) \quad (42)$$

In order to write the equations of motion eq.(42) we need to invert the Cauchy matrix. We find

$$(B^{-1})_{jp} = \frac{\prod_{l \neq p} (\epsilon_j - \lambda_l) \prod_i (\lambda_p - \epsilon_i)}{\prod_{i \neq j} (\epsilon_j - \epsilon_i) \prod_{l \neq p} (\lambda_p - \lambda_l)} \quad (43)$$

Hence

$$\partial_{t_i} \lambda_k = -i \frac{\sqrt{Q_{2n+2}(\lambda_k)}}{\prod_{l \neq k} (\lambda_k - \lambda_l)} \frac{\prod_{l \neq k} (\epsilon_i - \lambda_l)}{\prod_{j \neq i} (\epsilon_i - \epsilon_j)} \quad (44)$$

where the $-i$ comes from the symplectic form.

Note that we can also write equivalently

$$\sum_k B_{jk} \frac{1}{\mu_k} \partial_{t_i} \lambda_k = -i \delta_{ij}$$

where

$$\sigma_j(\lambda_k) = \frac{B_{kj}}{\mu_k} = \frac{\prod_{l \neq j} (\lambda_k - \epsilon_l)}{\sqrt{Q_{2n+2}(\lambda_k)}}$$

but $\sigma_j(\lambda) d\lambda$ are precisely a basis of holomorphic differentials. Hence we have

$$\sum_k \partial_{t_i} \lambda_k \sigma_j(\lambda_k) = -i \delta_{ij} \quad (45)$$

Define the angles as the images of the divisor (λ_k, μ_k) by the Abel map:

$$\theta_j = \sum_k \int^{\lambda_k} \sigma_j(\lambda, \mu) d\lambda$$

where $\sigma_j(\lambda, \mu) d\lambda$ is any basis of holomorphic differentials. This maps the dynamical divisor $(\lambda_k, \mu_k), k = 1 \cdots n$ to a point on the Jacobian of Γ . We can now prove the fundamental theorem of classical integrable systems

Theorem 1 *Under the above map, the flows generated by the Hamiltonians H_i are linear on the Jacobian.*

Proof. We want to show that the velocities $\partial_{t_i}\theta_j$ are constants, or

$$\partial_{t_i}\theta_j = \sum_k \partial_{t_i}\lambda_k \sigma_j(\lambda_k, \mu_k) = C_{ij}^{ste}$$

but this is eq.(45). ■

When the divisor (λ_k, μ_k) is in general position, the Jacobi inversion theorem [25] implies that the matrix $\sigma_j(\lambda_k)$ is invertible and therefore so is the matrix $\partial_{t_i}\lambda_k$. An important consequence of this fact is that the projections on the reduced system of the flows t_i are all independent as long as the spectral curve is non degenerate. In that case, the moment map is of rank $(n+1)$ if the orbit of H_{n+1} is one dimensional, or of rank n if the orbit of H_{n+1} is of dimension zero. But the flow generated by H_{n+1} is just a phase

$$b(t_{n+1}) = e^{it_{n+1}}b(0), \quad s_j^\pm(t_{n+1}) = e^{\pm it_{n+1}}s_j^\pm(0)$$

For the orbit of H_{n+1} to be of dimension zero we must have

$$b = \bar{b} = 0, \quad s_j^\pm = 0, \quad s_j^z = se_j, \quad e_j = \pm 1$$

and these are precisely the critical points where the rank of the moment map is zero. Outside these points the rank of the moment map of the full system is equal to the rank of the moment map of the reduced system plus one.

Let us assume that $Q_{2n+2}(\lambda)$ has a double *real* root at $\lambda = E$.

$$Q_{2n+2}(\lambda) = (\lambda - E)^2 \tilde{Q}_{2n}(\lambda)$$

This means that $A^2(\lambda) + B(\lambda)C(\lambda)$ has a double root. But for real λ one has $C(\lambda) = B^*(\lambda)$ so that $A(\lambda)$, $B(\lambda)$, $C(\lambda)$ must all vanish at $\lambda = E$.

Recalling eq.(36), this means² that one of the separated variables, say $\lambda_1(t)$, is frozen to E . This is compatible with eq.(44) which becomes

$$\partial_{t_i}\lambda_k = -i \frac{\sqrt{\tilde{Q}_{2n}(\lambda_k)}}{\prod_{l \neq k, 1} (\lambda_k - \lambda_l)} \frac{\prod_{l \neq k, 1} (\epsilon_i - \lambda_l)}{\prod_{j \neq i} (\epsilon_i - \epsilon_j)} (\epsilon_i - E), \quad k = 2 \dots n \quad (46)$$

These flows are not independent however. Because of the identities

$$\sum_{i=1}^n \frac{\epsilon_i^p}{\prod_{j \neq i} (\epsilon_i - \epsilon_j)} = 0, \quad 0 \leq p \leq n-2$$

² If $b(t) = \bar{b}(t) = 0$, then $B(\lambda)$ or $C(\lambda)$ are identically zero. The equation of motion $\partial_{t_j}b = igs_j^-$ implies $s_j^\pm(t) = 0$ and therefore $s_j^z(t) = se_j$. Hence this corresponds to the singular points.

we have the relation

$$\sum_i \frac{1}{\epsilon_i - E} \partial_{t_i} \lambda_k = 0, \quad k = 2 \cdots n$$

On this submanifold the rank of the moment map of the reduced system is therefore $n - 1$, and the moment map of the full system has rank n . By requiring more and more double zeroes and freezing more and more variables we construct the different strata of the moment map. This connection between degeneracies of the spectral curve and singularities of the momentum map has been exploited before for several integrable systems such as spinning tops [8].

In the case of a double *complex* root E , we do have solutions where one λ_k is frozen to E , but these do not exhaust all the corresponding fiber of the moment map. A detailed example of this is given in section 7 below, in the case of a system with one spin ($n = 1$).

We arrive at the interesting conclusion that the degeneracies of the moment map and the degeneracies of the spectral curve are intimately related. Recall that the spectral curve reads

$$\frac{Q_{2n+2}(\lambda)}{\prod(\lambda - \epsilon_i)^2} = 4\lambda^2 + 0\lambda + 4H_{n+1} + \sum_i \frac{2H_i}{\lambda - \epsilon_i} + \sum_i \frac{s^2}{(\lambda - \epsilon_i)^2} \quad (47)$$

The allowed real polynomials $Q_{2n+2}(\lambda)$ of degree $2n+2$ are characterized by the following conditions in the above expansion:

The coefficient of λ^2 is equal to four,

The coefficient of λ is equal to zero,

The coefficients of the double poles are $s^2 \implies Q_{2n+2}(\epsilon_i) = s^2 \prod_{j \neq i} (\epsilon_i - \epsilon_j)^2$

These are $n + 2$ conditions on the $2n + 3$ *real* coefficients of $Q_{2n+2}(\lambda)$. The remaining $n + 1$ coefficients are precisely the $n + 1$ Hamiltonians H_i . The degeneracies we look at are of the form

$$Q_{2n+2}(\lambda) = \left(\sum_{i=0}^{n+1-r} a_i \lambda^i \right)^2 \left(\sum_{j=0}^{2r} b_j \lambda^j \right)$$

where the coefficients a_i, b_j are *real*. The integer $0 \leq r \leq n + 1$ will be the rank of the moment map. To make the decomposition unique we can always impose $a_{n+1-r} = 1$ so that we have $(n + 1 - r) + 2r + 1 = n + r + 2$ coefficients on which we impose $n + 2$ constraints. Hence the leaf of rank r is of dimension r . We remark that the conditions we have to impose appear as linear equations on the b_j so that we always start by solving them. Another consequence of this remark is that if $2r > n + 1$ it remains $2r - n - 1$ free coefficients b_j which enter the problem linearly.

Hence the strata of rank r contain linear varieties of dimension $2r - n - 1$. In the cases of rank 0 and rank 1, the genus of the spectral curve is zero.

Strictly speaking, the rank can vary along a given fiber of the moment map. For example, let us consider a focus-focus critical point in an integrable system with two degrees of freedom. As we have already mentioned in section 4 the preimage of the critical value of the moment map is a torus which is pinched at the critical point. Therefore, the rank of the moment map for a generic point on this pinched torus is two, but it falls to zero at the critical point. The above prescription of freezing $n + 1 - r$ separated variables λ_k on double zeroes of Q_{2n+2} picks configurations which minimize the rank on the fiber of the moment map defined by the spectral curve.

7 The one-spin model.

We now study the example of the one-spin system from the point of view of the degeneracies of the spectral curve. This model is very well known in the physical literature [5] but also appeared recently in the mathematical literature [13]. In the one-spin case, the Hamiltonians read

$$\begin{aligned} H_1 &= 2\epsilon_1 s_1^z + b s_1^+ + \bar{b} s_1^- \\ H_2 &= \bar{b} b + s_1^z \end{aligned}$$

Recall again the spectral curve eq.(19) which reads in this case :

$$\frac{Q_4(\lambda)}{(\lambda - \epsilon_1)^2} = 4\lambda^2 + 4H_2 + 2\frac{H_1}{\lambda - \epsilon_1} + \frac{s^2}{(\lambda - \epsilon_1)^2} \quad (48)$$

We want to see when the spectral curve degenerates.

7.1 Rank 0:

As we have seen the singular points are given by $b = \bar{b} = 0$, $s_1^\pm = 0$. Hence we have two points

$$s_1^z = es, \quad e = \pm 1$$

The corresponding values $P = (H_1, H_2)$ are

$$P_1(\uparrow) = [2\epsilon_1 s, s]$$

$$P_2(\downarrow) = [-2\epsilon_1 s, -s]$$

We can recover this result by analysing the spectral curve. The most degenerate case is when $Q_4(\lambda)$ is a perfect square. Assuming

$$Q_4(\lambda) = (a_2 \lambda^2 + a_1 \lambda + a_0)^2, \quad a_2 \neq 0$$

We have three coefficients a_i on which we impose three conditions hence they are completely determined. We find

$$a_2\lambda^2 + a_1\lambda + a_0 = 2\left(\lambda^2 - \epsilon_1\lambda + \frac{s}{2}e_1\right)$$

Comparing the partial fraction decomposition of both sides of eq.(48), we find the corresponding values of (H_1, H_2) . They are precisely P_1 and P_2 . Hence the points of rank zero are the only points where the spectral curve is totally degenerate.

To determine the type of the singularities, we look at the classical Bethe equations which read

$$2\mu + \frac{se}{\mu - \epsilon_1} = 0 \Leftrightarrow 2\mu^2 - 2\epsilon_1\mu + se = 0$$

The discriminant of this equation is $\epsilon_1^2 - 2se$. So, when the spin is down (point P_2), the discriminant is positive, the two classical Bethe roots are real and this is an elliptic singularity, in agreement with the general analysis of section 4. When the spin is up (point P_1) we have real roots when $\epsilon_1^2 \geq 2s$ (i.e. the singularity is elliptic in this case), and a pair of complex conjugate roots E, \bar{E} when $\epsilon_1^2 \leq 2s$ (i.e. the singularity is focus-focus in that case).

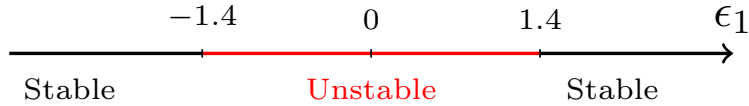


Figure 3: The domains of the coupling constant ϵ_1 , ($s = 1$).

Let us now discuss the fibers of the moment map over the critical values P_1 and P_2 . In the stable case, such fiber is reduced to the critical point. But in the unstable case (focus-focus singularity), this fiber is a two-dimensional torus pinched at the critical point. After the symplectic reduction associated to H_2 , the pinched torus is conveniently described as a finite arc in the complex plane of the separated variable λ_1 . The spectral polynomial can be written as:

$$Q_4(\lambda) = 4(\lambda - E)^2(\lambda - \bar{E})^2 \tag{49}$$

where:

$$\epsilon_1 = E + \bar{E}, \quad E\bar{E} = \frac{s}{2}$$

The separated variable λ_1 is defined by:

$$C(\lambda) = 2\bar{b} \frac{\lambda - \lambda_1}{\lambda - \epsilon_1} = 2\bar{b} + \frac{s_1^+}{\lambda - \epsilon_1}$$

so s_1^+ is expressed as:

$$s_1^+ = 2\bar{b}(\epsilon_1 - \lambda_1) \quad (50)$$

The conjugated variable μ_1 is equal to

$$\mu_1 = A(\lambda_1) = 2\lambda_1 + \frac{s_1^z}{\lambda - \epsilon_1}$$

so that:

$$s_1^z = (\epsilon_1 - \lambda_1)(2\lambda_1 - \mu_1) \quad (51)$$

Since (λ_1, μ_1) belongs to the spectral curve, we have:

$$\mu_1 = \pm 2 \frac{(\lambda_1 - E)(\lambda_1 - \bar{E})}{(\lambda_1 - \epsilon_1)}$$

Choosing the plus sign leads to $s_1^z = s$ which is the unstable point. So we now choose the minus sign, which gives:

$$s_1^z = -2(\lambda_1(\lambda_1 - E - \bar{E}) + (\lambda_1 - E)(\lambda_1 - \bar{E})) \quad (52)$$

The equation of motion for the flow generated by H_1 is:

$$\partial_{t_1} \lambda_1 = 2i(\lambda_1 - E)(\lambda_1 - \bar{E}) \quad (53)$$

whose solution is:

$$\lambda_1 = \frac{E - \bar{E}X}{1 - X}, \quad X = A_1 e^{2i(E - \bar{E})t_1}$$

From the expression of s_1^+ eq. (50) and the equation of motion

$$\partial_{t_1} \bar{b} = -is_1^+ \quad (54)$$

we deduce:

$$\bar{b}(t) = \bar{b}_0 \frac{e^{-2i\bar{E}t_1}}{1 - X}, \quad s_1^+ = 2\bar{b}_0 \frac{\bar{E} - EX}{(1 - X)^2} e^{-2i\bar{E}t_1}$$

From eq.(52) we get:

$$s_1^z = 2E\bar{E} - 4(E - \bar{E})^2 \frac{X}{(1 - X)^2}$$

Now s_1^z should be real, which is equivalent to $(X - \bar{X})(X\bar{X} - 1) = 0$. With $X = A_1 e^{2i(E - \bar{E})t_1}$ it is impossible to have $X\bar{X} = 1$ for all t_1 . Then $X = \bar{X}$, which imposes $\bar{A}_1 = A_1$ so that A_1 is real. Its

absolute value can be absorbed in the origin of time t_1 . Only its sign matters. To determine this sign, let us impose the constraint that the length of the spin is constant. This gives the condition:

$$\bar{b}_0 b_0 = 4A_1(E - \bar{E})^2$$

Then:

$$(s^z)^2 + s^+ s^- = 4E^2 \bar{E}^2 = s^2,$$

We see that A_1 should be negative. As a consequence, λ_1 runs along the line interval joining E and \bar{E} . Here, we see explicitly that freezing λ_1 on E (or on \bar{E}) gives only the critical point (\uparrow) which is only a tiny part of the fiber above the critical value P_1 in the focus-focus case. Note that on this fiber the rank of the moment map is two, excepted for the critical point (\uparrow) where it vanishes.

7.2 Rank 1

We assume next that

$$Q_4(\lambda) = (\lambda + a_0)^2(b_2\lambda^2 + b_1\lambda + b_0), \quad b_2 \neq 0 \quad (55)$$

where a_0 and b_i are real. We denote:

$$a_0 = \frac{1}{2}x - \epsilon_1$$

Imposing the three conditions on $Q_4(\lambda)$, we can determine b_0, b_1, b_2 in term of x by solving linear equations. We find:

$$b_2 = 4, \quad b_1 = -4x, \quad b_0 = 4 \frac{\epsilon_1 x^3 - \epsilon_1^2 x^2 + s^2}{x^2}$$

$$\begin{aligned} H_1 &= -\frac{x^4 - 2\epsilon_1 x^3 - 4s^2}{2x} \\ H_2 &= -\frac{3x^4 - 8\epsilon_1 x^3 + 4\epsilon_1^2 x^2 - 4s^2}{4x^2} \end{aligned}$$

and we see that:

$$\frac{\partial H_1}{\partial x} = x \frac{\partial H_2}{\partial x} \quad (56)$$

Since we are on a rank one line, the derivatives of the functions H_1, H_2 with respect to any coordinates X and Y on phase space, evaluated on the line are proportional:

$$\frac{\partial}{\partial X} \begin{pmatrix} H_1 \\ H_2 \end{pmatrix} \propto \frac{\partial}{\partial Y} \begin{pmatrix} H_1 \\ H_2 \end{pmatrix} \implies \frac{\partial_X H_1}{\partial_X H_2} = \frac{\partial_Y H_1}{\partial_Y H_2} = x$$

In particular we have:

$$\frac{\partial H_1}{\partial b} = x \frac{\partial H_2}{\partial b} \implies s_1^+ = x\bar{b}$$

Inserting this relation into the definitions of H_1 and H_2 gives: $H_2 = \bar{b}b + s_1^z$ and $H_1 = 2\epsilon_1 s_1^z + 2x\bar{b}b$. Therefore:

$$s_1^z = -\frac{1}{2}x(x - 2\epsilon_1)$$

$$\bar{b}b = \frac{(2s - x^2 + 2\epsilon_1 x)(2s + x^2 - 2\epsilon_1 x)}{4x^2}$$

Notice that when

$$x^2 - 2\epsilon_1 x + 2es = 0, \quad e = \pm 1 \quad (57)$$

we have $s_1^z = es$ and $\bar{b}b = 0$ and this corresponds to the points P_1 and P_2 . In fact there is a simple relation between rank 0 and rank 1. Rank 1 spectral curves degenerate when the polynomial $b_2\lambda^2 + b_1\lambda + b_0$ has a double real root. Its discriminant is:

$$b_1^2 - 4b_0b_2 = 16 \frac{(x^2 - 2\epsilon_1 x - 2s)(x^2 - 2\epsilon_1 x + 2s)}{x^2} = -64 \bar{b}b \leq 0$$

It vanishes precisely when eqs.(57) are satisfied. These equations are nothing but the classical Bethe equations eq.(26) as can be seen by setting

$$x = 2\mu$$

Remark that the boundary of the image of the moment map is obtained for x real, because H_1 and H_2 are both real. Hence the elliptic points are on the boundary, but the focus-focus points correspond to complex x and therefore are not on this boundary (see fig. 7 below). To end the characterization of the boundary of the moment map we have to determine the range of x . The physical constraints are $-s \leq s_1^z \leq s$ and $\bar{b}b \geq 0$. These two conditions are both equivalent to:

$$-2s + \epsilon_1^2 \leq (x - \epsilon_1)^2 \leq 2s + \epsilon_1^2 \quad (58)$$

In this inequality we recognize the discriminants $\epsilon_1^2 \pm 2s$ of the classical Bethe equations, so that we have to distinguish between the stable and unstable case.

7.2.1 Stable case.

When $\epsilon_1^2 \geq 2s$ the two sides of the inequality are positive and put bounds on x . The two equations determining the boundary values of x are precisely eqs.(57), and we are in the case where all their roots are real. The allowed range of x is as in fig.(4). From this we can construct the image of the moment map. It is shown in fig.(5) with the edges labelled according to the ranges of x . The point P_2 (spin down) is the green point and the point P_1 (spin up) is the cyan point. They are both on the boundary of the image.

The swallow tail is not part of the image of the moment map. It is composed of the points $(H_1(x), H_2(x))$ when x runs in the interval $[\epsilon_1 - \sqrt{-2s + \epsilon_1^2}, \epsilon_1 + \sqrt{-2s + \epsilon_1^2}]$. The two cusps

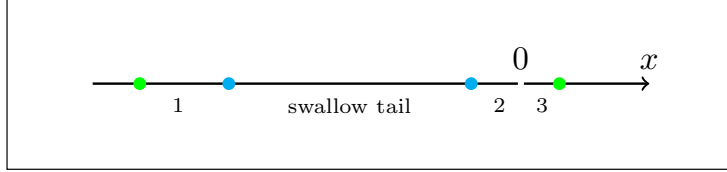


Figure 4: The range of x . The allowed segments are labelled 1, 2, 3. The points of the same color are mapped to the same singular point in the bifurcation diagram. Notice that $x = 0$ is mapped to infinity. ($\epsilon_1 = -2$).

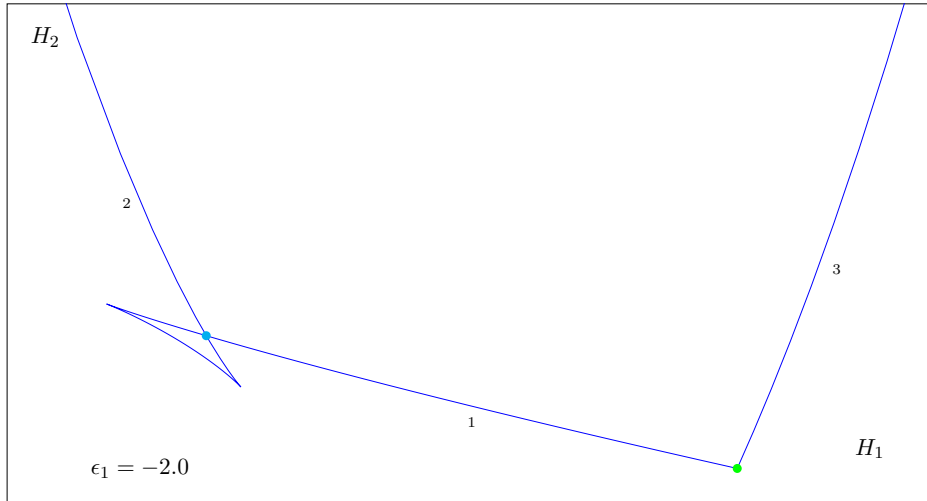


Figure 5: Image of the moment map in the stable case. The swallow tail is not part of the image of the moment map. ($\epsilon_1 = -2$).

correspond to values x_c of x such that $\partial H_1/\partial x$ and $\partial H_2/\partial x$ both vanish. Let us write $x = x_c + u$. Then, taking into account eq. (56), we have the following Taylor expansions for small u :

$$\delta H_2 = \frac{\alpha}{2}u^2 + \frac{\beta}{3}u^3 + \mathcal{O}(u^4) \quad (59)$$

$$\delta H_1 = x_c \delta H_2 + \frac{\alpha}{3} u^3 + \mathcal{O}(u^4) \quad (60)$$

where δH_i stands for the the small variation $H_i(x_c + u) - H_i(x_c)$. From eq. (59), we have:

$$u = \pm \left(\frac{2}{\alpha} |\delta H_2| \right)^{1/2} + \mathcal{O}(\delta H_2)$$

Therefore:

$$\delta H_1 = x_c \delta H_2 \pm \frac{\alpha}{3} \left(\frac{2}{\alpha} |\delta H_2| \right)^{3/2} + \mathcal{O}((\delta H_2)^2) \quad (61)$$

which gives the leading shape of the cusp near x_c . We see that the two branches are found on opposite sides of their common tangent, as shown on fig. 5.

7.2.2 Unstable case.

When $\epsilon_1^2 \leq 2s$ the left side of the inequality (58) is always satisfied. Among the equations eqs.(57) determining the bounds of x , one has two real roots and the other one has two complex conjugate roots. The range of x is as in fig.(6). The image of the moment map is shown in fig.(7). The point P_2 (spin down) is the green point and is a vertex on the boundary. The point P_1 (spin up) is the red point. It is in the interior of the image of the moment map.

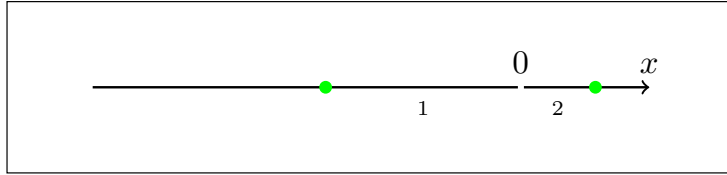


Figure 6: The range of x . The green points correspond to the stable point P_2 and are solutions of the equation $x^2 - 2\epsilon_1 x - 2s = 0$. Since points of the same color are mapped to the same point by the moment map, and zero is mapped to ∞ , the boundaries of the image of this map are easy to reconstruct. ($\epsilon_1 = -0.707$).

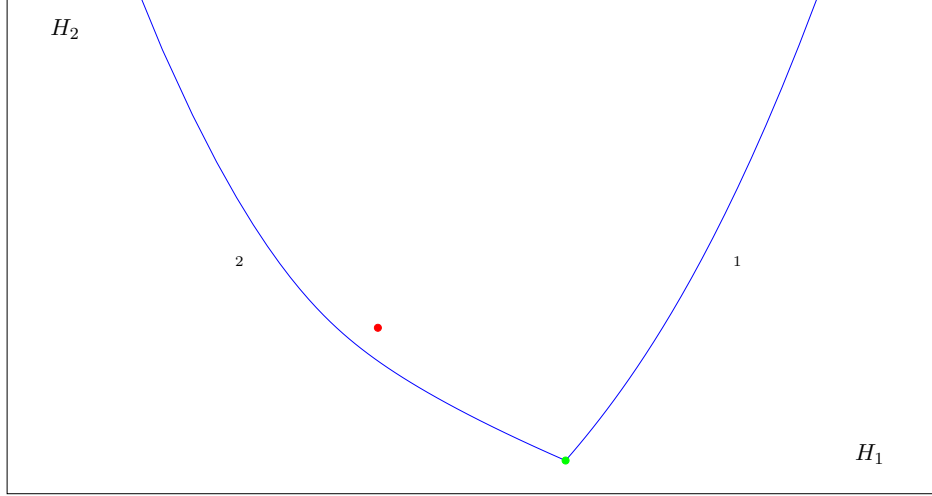


Figure 7: The image of the moment map in the case of one spin, with one unstable critical point. The green point is the stable (elliptic) point P_2 . The red point is the unstable (focus-focus) point P_1 . It is in the interior of the image of the moment map. ($\epsilon_1 = -0.707$).

8 The two-spins model.

For the two spins model, let us write explicitly the Hamiltonians:

$$\begin{aligned} H_1 &= 2\epsilon_1 s_1^z + b s_1^+ + \bar{b} s_1^- + \frac{s_1 \cdot s_2}{\epsilon_1 - \epsilon_2} \\ H_2 &= 2\epsilon_2 s_2^z + b s_2^+ + \bar{b} s_2^- - \frac{s_1 \cdot s_2}{\epsilon_1 - \epsilon_2} \\ H_3 &= \bar{b} b + s_1^z + s_2^z \end{aligned}$$

where

$$s_1 \cdot s_2 = s_1^z s_2^z + \frac{1}{2}(s_1^- s_2^+ + s_1^+ s_2^-)$$

The spectral curve reads in this case:

$$\frac{Q_6(\lambda)}{(\lambda - \epsilon_1)^2 (\lambda - \epsilon_2)^2} = 4\lambda^2 + 4H_3 + \frac{2H_1}{\lambda - \epsilon_1} + \frac{2H_2}{\lambda - \epsilon_2} + \frac{s^2}{(\lambda - \epsilon_1)^2} + \frac{s^2}{(\lambda - \epsilon_2)^2} \quad (62)$$

Let us now use the degeneracies of zeroes of $Q_6(\lambda)$ to study the rank of the moment map.

8.1 Rank 0

Again, the singular points are given by $b = \bar{b} = 0$, $s_1^\pm = s_2^\pm = 0$ so that we have four critical points:

$$s_1^z = \pm s, \quad s_2^z = \pm s$$

The corresponding values $P = (H_1, H_2, H_3)$ are:

$$P_1(\uparrow, \uparrow) = \left[\frac{s^2}{\epsilon_1 - \epsilon_2} + 2\epsilon_1 s, \quad 2\epsilon_2 s - \frac{s^2}{\epsilon_1 - \epsilon_2}, \quad 2s \right] \quad (63)$$

$$P_2(\uparrow, \downarrow) = \left[2\epsilon_1 s - \frac{s^2}{\epsilon_1 - \epsilon_2}, \quad \frac{s^2}{\epsilon_1 - \epsilon_2} - 2\epsilon_2 s, \quad 0 \right] \quad (64)$$

$$P_3(\downarrow, \uparrow) = \left[-2\epsilon_1 s - \frac{s^2}{\epsilon_1 - \epsilon_2}, \quad \frac{s^2}{\epsilon_1 - \epsilon_2} + 2\epsilon_2 s, \quad 0 \right] \quad (65)$$

$$P_4(\downarrow, \downarrow) = \left[\frac{s^2}{\epsilon_1 - \epsilon_2} - 2\epsilon_1 s, \quad -2\epsilon_2 s - \frac{s^2}{\epsilon_1 - \epsilon_2}, \quad -2s \right] \quad (66)$$

We can recover this result by analysing the degeneracies of the spectral curve. The most degenerate case corresponds to a polynomial $Q_6(\lambda)$ of the form

$$Q_6(\lambda) = (a_3\lambda^3 + a_2\lambda^2 + a_1\lambda + a_0)^2$$

The four conditions we have to impose on $Q_6(\lambda)$ determine completely the four coefficients a_i . We find:

$$a_3\lambda^3 + a_2\lambda^2 + a_1\lambda + a_0 = 2 \left(\lambda^3 - (\epsilon_1 + \epsilon_2)\lambda^2 + \left(\epsilon_1\epsilon_2 + \frac{s}{2}(e_1 + e_2) \right) \lambda - \frac{s}{2}(e_1\epsilon_2 + e_2\epsilon_1) \right) \quad (67)$$

where $e_i = \pm 1$. The values of the energies are exactly eqs.(63–66).

In order to determine the type of the singularities we write the classical Bethe equations:

$$2\mu + \frac{s\epsilon_1}{\mu - \epsilon_1} + \frac{s\epsilon_2}{\mu - \epsilon_2} = 0 \quad (68)$$

These are polynomial equations of degree 3. The number of real roots is determined by the sign of the discriminant:

$$\begin{aligned} \text{Disc}(e_1, e_2) &= -4\epsilon_1^2\epsilon_2^2(\epsilon_2 - \epsilon_1)^2 + 4(\epsilon_2 - \epsilon_1)(2e_1\epsilon_2^3 + e_2\epsilon_1\epsilon_2^2 - 2e_1\epsilon_1\epsilon_2^2 + 2e_2\epsilon_1^2\epsilon_2 - e_1\epsilon_1^2\epsilon_2 - 2e_2\epsilon_1^3)s \\ &\quad - (\epsilon_2^2 + 20e_1e_2\epsilon_2^2 - 8\epsilon_2^2 + 8\epsilon_1\epsilon_2 - 38e_1e_2\epsilon_1\epsilon_2 + 8\epsilon_1\epsilon_2 - 8\epsilon_1^2 + 20e_1e_2\epsilon_1^2 + \epsilon_1^2)s^2 \\ &\quad + 2(e_2 + e_1)^3s^3 \end{aligned}$$

If $\text{Disc}(e_1, e_2) < 0$ we have three real roots (elliptic point) and if $\text{Disc} > 0$ we have one real root (focus-focus singularity). We restrict ourselves to the case where ϵ_1 and ϵ_2 are both negative. We

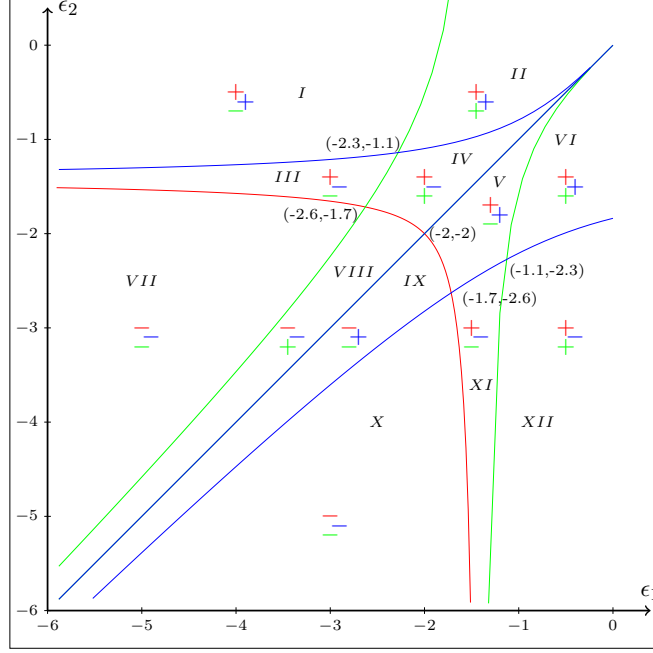


Figure 8: The domains indicating the signs of the various discriminants, for three critical points of the system with two spins. Curves correspond to the vanishing of one discriminant. The color of these curves and of signs inside the domains label the critical points according to the following code: red stands for up-up, green for up-down, and blue for down-up. ($s = 1$).

easily see that $\text{Disc}(e_1 = -1, e_2 = -1)$ is always negative, hence the configuration with two spins down is always stable. The signs of the other three discriminants is shown in fig.(8).

In region V , for instance, we have two unstable points and two stable points.

- (\uparrow, \uparrow) : one real root (unstable)
- (\uparrow, \downarrow) : three real roots (stable)
- (\downarrow, \uparrow) : one real root (unstable)
- (\downarrow, \downarrow) : three real roots (always stable)

8.2 Rank 1

We now set

$$Q_6(\lambda) = (\lambda^2 + a_1\lambda + a_0)^2(b_2\lambda^2 + b_1\lambda + b_0) \quad (69)$$

We have five coefficients and four conditions on Q_6 . Hence we have a dimension one manifold of solutions. The coefficients b_j are completely determined and there is one constraint between (a_0, a_1) . Note that the case of rank 0 is obtained as a special case of rank 1, when the polynomial $b_2\lambda^2 + b_1\lambda + b_0$ has a doubly degenerate root. Let us parametrize (a_0, a_1) in terms of (x, y) as follows:

$$a_0 = -\frac{\epsilon_1 y + \epsilon_2 x - 2\epsilon_1 \epsilon_2}{2}, \quad a_1 = \frac{y + x - 2\epsilon_2 - 2\epsilon_1}{2}$$

Imposing the coefficient of λ^2 we find:

$$b_2 = 4$$

Imposing the vanishing of the coefficient of λ , we find:

$$b_1 = -4(y + x)$$

Imposing that the coefficient of the double pole at $\lambda = \epsilon_2$ is s^2 we find:

$$b_0 = \frac{4(\epsilon_2 y^3 + \epsilon_2 x y^2 - \epsilon_2^2 y^2 + s^2)}{y^2}$$

Imposing next that the coefficient of the double pole at $\lambda = \epsilon_1$ is s^2 we find the constraint:

$$S_1 : s^2(y^2 - x^2) + (\epsilon_1 - \epsilon_2)(x + y - \epsilon_1 - \epsilon_2)x^2 y^2 = 0 \quad (70)$$

Then H_1, H_2, H_3 are given by eqs.(71,72,73).

$$\begin{aligned} H_1 = & \frac{1}{2(\epsilon_2 - \epsilon_1)y^2} ((\epsilon_2 - \epsilon_1)(-2xy^4 - 3x^2y^3 - 2(-3\epsilon_2 + \epsilon_1)xy^3 - x^3y^2) \\ & - (\epsilon_2 - \epsilon_1)(-4\epsilon_2 + 2\epsilon_1)x^2y^2 + 4(\epsilon_2 - \epsilon_1)^2(-\epsilon_2 - \epsilon_1)xy^2 - 2s^2xy \\ & + 4(\epsilon_2 - \epsilon_1)s^2x) \end{aligned} \quad (71)$$

$$H_2 = \frac{-(\epsilon_2 - \epsilon_1)y^4 - (\epsilon_2 - \epsilon_1)xy^3 - (\epsilon_2 - \epsilon_1)(-2\epsilon_2)y^3 + 2s^2x + 4\epsilon_2s^2 - 4\epsilon_1s^2}{2(\epsilon_2 - \epsilon_1)y} \quad (72)$$

$$H_3 = \frac{-3y^4 - 6xy^3 - 4(-2\epsilon_2)y^3 - 3x^2y^2 - 4(-\epsilon_2 - \epsilon_1)xy^2 - (-2\epsilon_2)^2y^2 + 4s^2}{4y^2} \quad (73)$$

These are the parametric equations of the lines of rank 1. The parameters x and y are tied together by relation eq.(70).

Let us now define the total derivative with respect to x by:

$$\frac{d}{dx} = \frac{\partial}{\partial x} + \frac{dy}{dx} \frac{\partial}{\partial y}, \quad \text{where } \frac{dy}{dx} = -\frac{\partial_x S_1}{\partial_y S_1}$$

Then we can compute:

$$\begin{aligned} \frac{dH_1}{dx} - x \frac{dH_3}{dx} &= -\frac{y + 2(\epsilon_1 - \epsilon_2)}{(\epsilon_1 - \epsilon_2)xy^3} \frac{dy}{dx} S_1 \\ \frac{dH_2}{dx} - y \frac{dH_3}{dx} &= \frac{2}{(\epsilon_1 - \epsilon_2)xy^2} \frac{dy}{dx} S_1 \end{aligned}$$

hence, on S_1 , we have:

$$\frac{dH_1}{dx} = x \frac{dH_3}{dx}, \quad \frac{dH_2}{dx} = y \frac{dH_3}{dx}$$

Because we are on a rank one line this relation is true for any derivative on the line. Considering the derivative with respect to b we find

$$s_1^+ = x\bar{b}, \quad s_2^+ = y\bar{b}$$

and considering the derivative with respect to s_1^+ we get:

$$2s_1^z + \frac{1}{\epsilon_1 - \epsilon_2}(-xs_2^z + ys_1^z) = -x^2 + 2\epsilon_1 x, \quad \frac{1}{\epsilon_1 - \epsilon_2}(-xs_2^z + ys_1^z) = xy$$

from which we deduce:

$$s_1^z = -\frac{x}{2}(x + y - 2\epsilon_1), \quad s_2^z = -\frac{y}{2}(x + y - 2\epsilon_2)$$

and:

$$\bar{b}b = -\frac{(y^2 + xy - 2\epsilon_2 y - 2s)(y^2 + xy - 2\epsilon_2 y + 2s)}{4y^2}$$

Note that the discriminants of the two second degree polynomials which appear in the factorization (69) of $Q_6(\lambda)$ are:

$$\begin{aligned} b_1^2 - 4b_0b_2 &= \frac{16(y(x+y) - 2\epsilon_2 y - 2s)(y(x+y) - 2\epsilon_2 y + 2s)}{y^2} = -64\bar{b}b < 0 \\ a_1^2 - 4a_0 &= \frac{1}{4} \left((x+y)^2 - 4(\epsilon_1 - \epsilon_2)(x-y) + 4(\epsilon_1 - \epsilon_2)^2 \right) \equiv \frac{1}{4} \Delta \end{aligned}$$

The first discriminant vanishes when $Q_6(\lambda)$ has three double roots, that is when the rank drops to zero. In this case, inserting the parametrization

$$x = -s \frac{e_1}{\mu - \epsilon_1}, \quad y = -s \frac{e_2}{\mu - \epsilon_2}$$

into eq.(70), we see that it turns into the classical Bethe equation for μ . The variables x, y being real by definition, the real solutions of the classical Bethe equations correspond to points on the curve S_1 .

When $\Delta > 0$, $Q_6(\lambda)$ has two real double roots, which become a pair of complex conjugated double roots when $\Delta < 0$. Most likely, the sign of Δ governs the nature of the preimage of points lying on such a line of rank 1. To check this, one would need to compute the corresponding normal forms, which we have not done yet, the normal forms discussed previously being specialized to the special case of rank zero singular points. We leave this generalization as a subject for future work. We expect that points where $\Delta = 0$ correspond to qualitative changes in the topology of the pre-image. They are determined by the following factorization for $Q_6(\lambda)$:

$$Q_6(\lambda) = 4(\lambda - a_0)^4(\lambda^2 + b_1\lambda + b_0)$$

As before, we express the known constraints on this polynomial, which gives:

$$\begin{aligned} 4(-a_0 + \epsilon_1)^4 (b_0 + b_1 \epsilon_1 + \epsilon_1^2) - (\epsilon_1 - \epsilon_2)^2 s^2 &= 0 \\ 4(-a_0 + \epsilon_2)^4 (b_0 + b_1 \epsilon_2 + \epsilon_2^2) - (\epsilon_1 - \epsilon_2)^2 s^2 &= 0 \\ -16 a_0 + 4 b_1 + 8 \epsilon_1 + 8 \epsilon_2 &= 0 \end{aligned}$$

Solving for b_0 and b_1 in the first two equations gives:

$$b_0 = \epsilon_1 \epsilon_2 - \frac{(-\epsilon_1^2 + \epsilon_1 \epsilon_2) s^2}{4 (a_0 - \epsilon_2)^4} + \frac{(-\epsilon_1 \epsilon_2 + \epsilon_2^2) s^2}{4 (a_0 - \epsilon_1)^4}$$

and

$$b_1 = -\epsilon_1 - \epsilon_2 - \frac{(-\epsilon_1 + \epsilon_2) s^2}{4 (a_0 - \epsilon_1)^4} + \frac{(-\epsilon_1 + \epsilon_2) s^2}{4 (a_0 - \epsilon_2)^4}$$

Plugging these values in the third equation determines a_0 through:

$$-16 a_0 + 4 \epsilon_1 + 4 \epsilon_2 + \frac{(\epsilon_1 - \epsilon_2) s^2}{(a_0 - \epsilon_1)^4} + \frac{(-\epsilon_1 + \epsilon_2) s^2}{(a_0 - \epsilon_2)^4} = 0$$

8.3 Rank 2

We now set:

$$Q_6(\lambda) = (\lambda + a_0)^2(b_4\lambda^4 + b_3\lambda^3 + b_2\lambda^2 + b_1\lambda + b_0) \quad (74)$$

The four constraints are linear equations determining b_4, b_3, b_2, b_1 . It remains two parameters a_0, b_0 . The rank 2 manifolds are two-dimensional surfaces. Remark that b_0 appears linearly. The four conditions on Q_6 read:

$$\begin{aligned} b_4 &= 4 \\ (\epsilon_1 + a_0)^2 (b_4 \epsilon_1^4 + b_3 \epsilon_1^3 + b_2 \epsilon_1^2 + b_1 \epsilon_1 + b_0) &= (\epsilon_1 - \epsilon_2)^2 s^2 \\ (\epsilon_2 + a_0)^2 (b_4 \epsilon_2^4 + b_3 \epsilon_2^3 + b_2 \epsilon_2^2 + b_1 \epsilon_2 + b_0) &= (\epsilon_1 - \epsilon_2)^2 s^2 \\ 2b_4 \epsilon_2 + 2b_4 \epsilon_1 + 2a_0 b_4 + b_3 &= 0 \end{aligned}$$

We can solve them in terms of a_0 and b_0 :

$$\begin{aligned} b_4 &= 4 \\ b_3 &= -8(\epsilon_2 + \epsilon_1 + a_0) \\ b_2 &= \frac{(\epsilon_2 - \epsilon_1) s^2}{\epsilon_2 (\epsilon_2 + a_0)^2} - \frac{(\epsilon_2 - \epsilon_1) s^2}{\epsilon_1 (\epsilon_1 + a_0)^2} + \frac{4\epsilon_1 \epsilon_2^3 + a_0 (8\epsilon_1 \epsilon_2^2 + 8\epsilon_1^2 \epsilon_2) + 12\epsilon_1^2 \epsilon_2^2 + 4\epsilon_1^3 \epsilon_2 + b_0}{\epsilon_1 \epsilon_2} \\ b_1 &= \frac{(\epsilon_2^2 - \epsilon_1 \epsilon_2) s^2}{\epsilon_1 (\epsilon_1 + a_0)^2} - \frac{(\epsilon_1 \epsilon_2 - \epsilon_1^2) s^2}{\epsilon_2 (\epsilon_2 + a_0)^2} - \frac{4\epsilon_1^2 \epsilon_2^3 + 4\epsilon_1^3 \epsilon_2^2 + 8a_0 \epsilon_1^2 \epsilon_2^2 + b_0 \epsilon_2 + b_0 \epsilon_1}{\epsilon_1 \epsilon_2} \end{aligned}$$

Once these constraints are implemented, we can write the Hamiltonians on the faces of the image of the moment map, which are therefore parametrized by a_0 and b_0 :

$$\begin{aligned} H_1 &= \frac{(\epsilon_2^2 + \epsilon_1^2) s^2 + a_0 (8\epsilon_1^3 \epsilon_2^2 + 8\epsilon_1^4 \epsilon_2 - 2b_0 \epsilon_1) + a_0^2 (4\epsilon_1^2 \epsilon_2^2 + 16\epsilon_1^3 \epsilon_2 - b_0) + 4\epsilon_1^4 \epsilon_2^2 + 8a_0^3 \epsilon_1^2 \epsilon_2 - b_0 \epsilon_1^2}{2\epsilon_1 \epsilon_2^2 - 2\epsilon_1^2 \epsilon_2} \\ &\quad - \frac{\epsilon_1 s^2}{\epsilon_2 (\epsilon_2 + a_0)} + \frac{(\epsilon_1 \epsilon_2 - \epsilon_1^2) s^2}{2\epsilon_2 (\epsilon_2 + a_0)^2} + \frac{s^2}{\epsilon_1 + a_0} \\ H_2 &= -\frac{(\epsilon_2^2 + \epsilon_1^2) s^2 + a_0 (8\epsilon_1 \epsilon_2^4 + 8\epsilon_1^2 \epsilon_2^3 - 2b_0 \epsilon_2) + 4\epsilon_1^2 \epsilon_2^4 + a_0^2 (16\epsilon_1 \epsilon_2^3 + 4\epsilon_1^2 \epsilon_2^2 - b_0) + 8a_0^3 \epsilon_1 \epsilon_2^2 - b_0 \epsilon_2^2}{2\epsilon_1 \epsilon_2^2 - 2\epsilon_1^2 \epsilon_2} \\ &\quad + \frac{s^2}{\epsilon_2 + a_0} - \frac{(\epsilon_2^2 - \epsilon_1 \epsilon_2) s^2}{2\epsilon_1 (\epsilon_1 + a_0)^2} - \frac{\epsilon_2 s^2}{\epsilon_1 (\epsilon_1 + a_0)} \\ H_3 &= \frac{(\epsilon_2 - \epsilon_1) s^2}{4\epsilon_2 (\epsilon_2 + a_0)^2} - \frac{(\epsilon_2 - \epsilon_1) s^2}{4\epsilon_1 (\epsilon_1 + a_0)^2} - \frac{a_0 (8\epsilon_1 \epsilon_2^2 + 8\epsilon_1^2 \epsilon_2) + 4\epsilon_1^2 \epsilon_2^2 + 12a_0^2 \epsilon_1 \epsilon_2 - b_0}{4\epsilon_1 \epsilon_2} \end{aligned}$$

Remark that b_0 enters the formulae linearly so that the rank two faces are ruled surfaces. To find the intersection between two faces, we go back to eq.(69). As we have seen, the discriminant $b_1^2 - 4b_0b_2 = -64\bar{b}b$ is zero at a critical point and negative as soon as we leave this critical point. So the double real root at a critical point splits into a pair of complex conjugate roots as soon as we move along the rank 1 line. If the other discriminant $a_1^2 - 4a_0 = (1/4)\Delta$ is positive, the polynomial $\lambda^2 + a_1\lambda + a_0$ has real roots α_1 and α_2 , and we can recast Q_6 as $Q_6(\lambda) = (\lambda - \alpha_1)^2((\lambda - \alpha_2)^2(\tilde{b}_2\lambda^2 + \tilde{b}_1\lambda + \tilde{b}_0))$. Expanding the second factor (of degree four), we obtain an expression of the form (74) with *real* coefficients, which satisfies all the constraints. This establishes that the line of rank one, defined by eq.(69) is included in a face of rank two, as long as the roots α_1 and α_2 are real, that is when $\Delta > 0$. When Δ crosses zero to become negative, the line of rank one starts to leave the face and goes inside the image of the moment map. The corresponding roots form a complex conjugated pair of double roots.

We have also established that the points of rank zero are on the faces as well as the edges of rank one, provided $\Delta > 0$. This last condition excludes the lines of rank 1 which go in the interior of the image of the moment map when $\Delta < 0$.

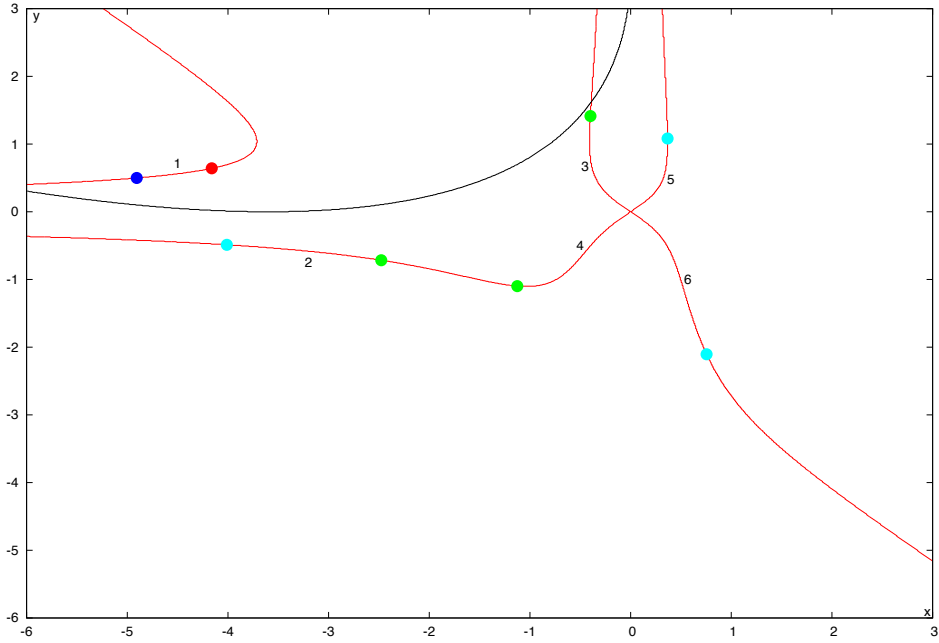


FIGURE 9. The curve $S1$ for a point in region I . The red and blue points correspond to the unstable points P_1 and P_3 respectively. The green and cyan points correspond to the stable points P_2 and P_4 respectively. Since points of the same color are mapped to the same point by the moment map, the edges of the image of the moment map are easy to reconstruct. The black curve corresponds to $\Delta = 0$. The origin has $\Delta > 0$. We see that the edge joining the unstable points is not on the faces. ($\epsilon_1 = -2, \epsilon_2 = -0.2$).

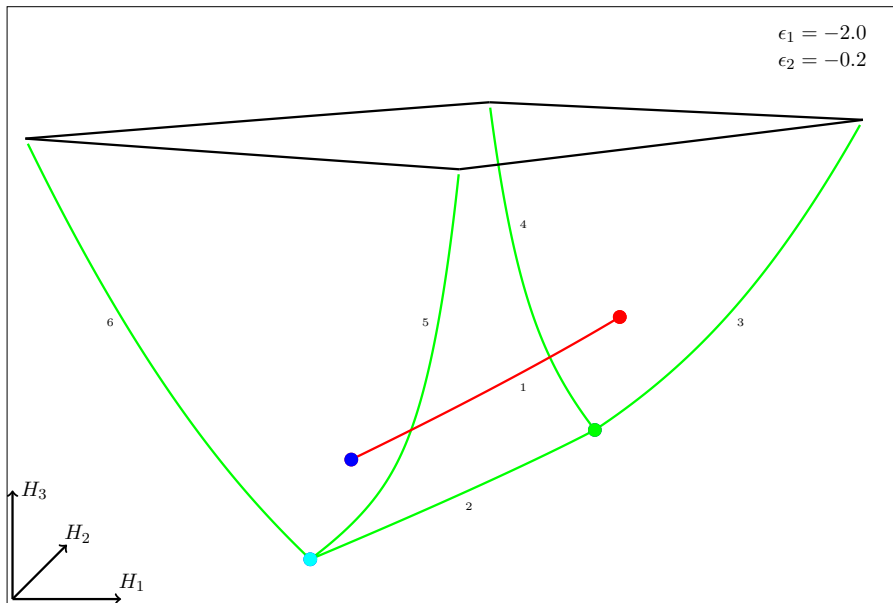


FIGURE 10. The image of the moment map (IMM) and the bifurcation diagram for a point in region I . It has four faces. The stable points are vertices of the IMM. The unstable points are on and inside faces. A line of rank 1 joins the red point to the blue point passing inside the IMM. ($\epsilon_1 = -2, \epsilon_2 = -0.2$).

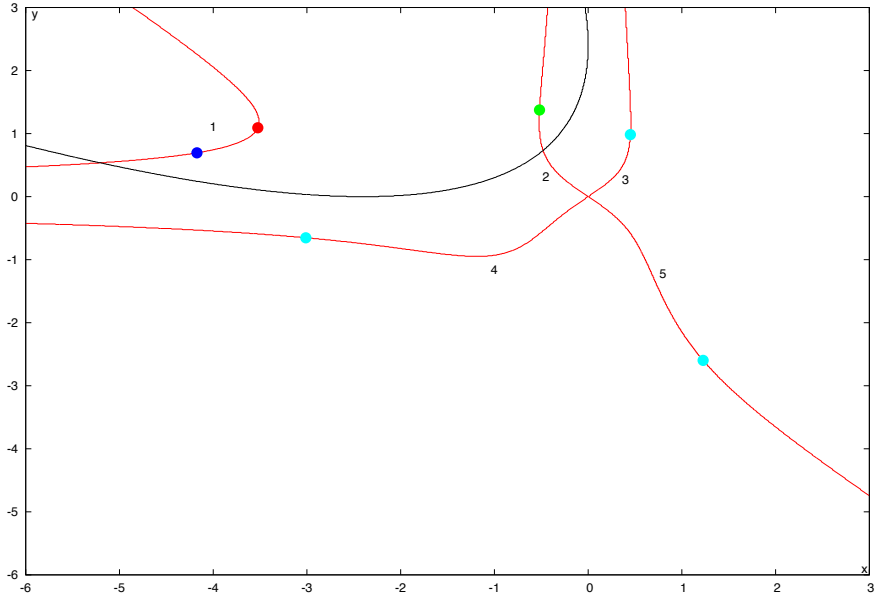


FIGURE 11. The curve S_1 for a point in region II . The red, green, and blue points correspond to the unstable points P_1 , P_2 and P_3 respectively. The cyan points correspond to the stable point P_4 . Since points of the same color are mapped to the same point by the moment map, the edges of the IMM are easy to reconstruct. The black curve corresponds to $\Delta = 0$. The origin has $\Delta > 0$. We see that the edge joining the unstable points is not on the faces. Note that the arc joining P_2 (green point) to the origin (point at infinity in the IMM) crosses the $\Delta = 0$ curve. ($\epsilon_1 = -1.5, \epsilon_2 = -0.3$).

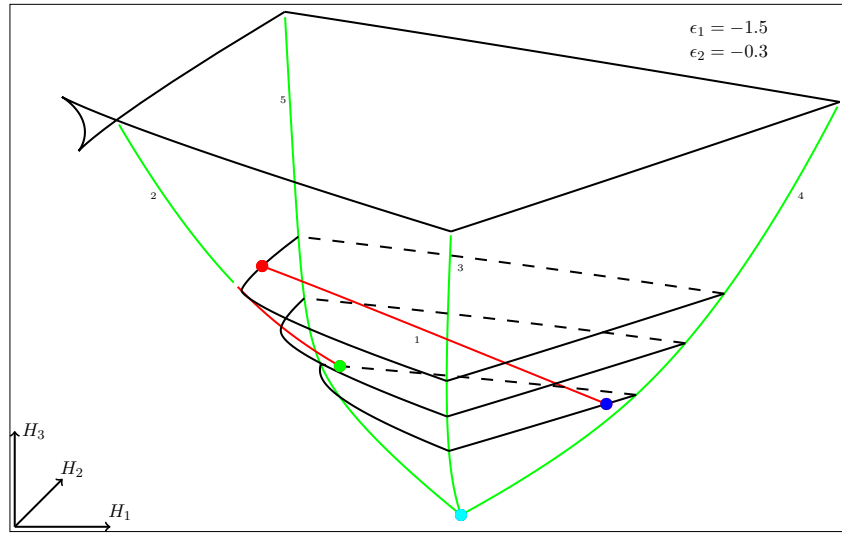


FIGURE 12. The IMM and the bifurcation diagram for a point in region II . The stable point is the vertex of the IMM. The unstable points are on and inside faces. A line of rank 1 joins the red point to the blue point passing inside the IMM. Another line joins the unstable point P_2 (green) to infinity. Starting from P_2 , it runs inside the IMM and later becomes an edge between two faces as the discriminant Δ becomes positive. This is a consequence of the crossing between the $\Delta = 0$ curve and line 2 shown on the previous figure. ($\epsilon_1 = -1.5, \epsilon_2 = -0.3$).

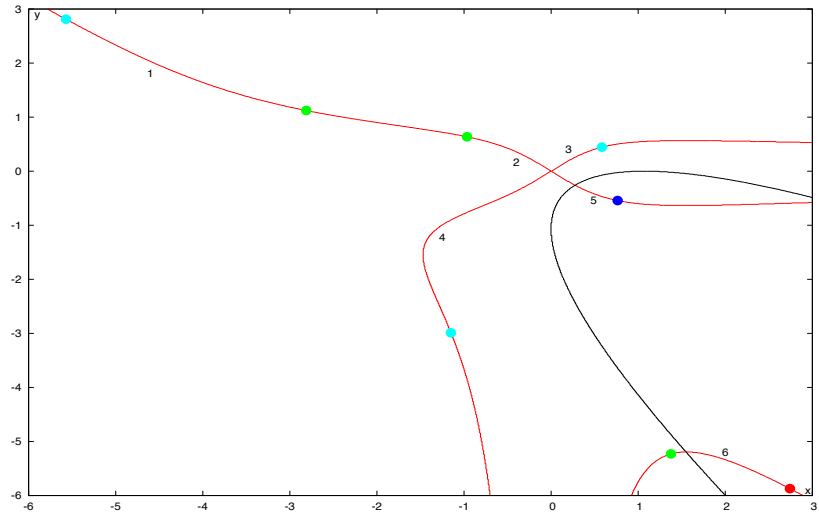


FIGURE 13. The curve S_1 for a point in region V . The red and blue points correspond to the unstable points P_1 and P_3 respectively. The green and cyan points correspond to the stable points P_2 and P_4 respectively. Since points of the same color are mapped to the same point by the moment map, the edges of the IMM are easy to reconstruct. The black curve corresponds to $\Delta = 0$. The origin has $\Delta > 0$. We see that the two edges starting from the unstable points are not on the faces, but they will join the faces when Δ becomes > 0 . ($\epsilon_1 = -1.2, \epsilon_2 = -1.735$).

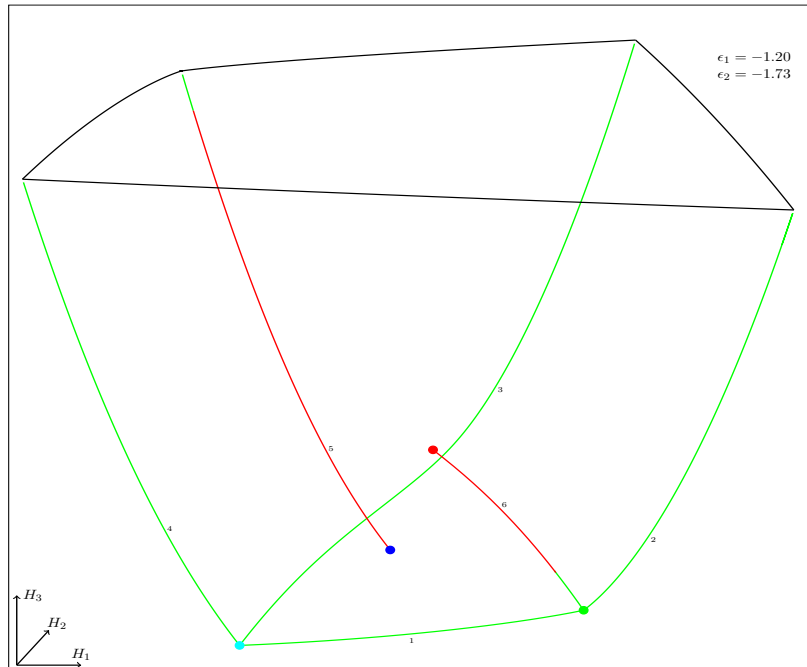


FIGURE 14. The IMM and the bifurcation diagram for a point in region V . The stable points are vertices of the IMM. The unstable points are on and inside faces. A line of rank 1 joins the red point P_1 to the green vertex P_2 . In the vicinity of P_1 , it runs inside the IMM. But as shown on the previous figure, Δ changes sign along this line (where the color changes from green to red) before reaching P_2 . When Δ is positive, this line becomes an edge separating two faces. Another line of rank 1 joins the blue point P_3 to infinity, passing inside the IMM in the vicinity of P_3 , and becoming later an edge between two faces. ($\epsilon_1 = -1.2, \epsilon_2 = -1.735$).

9 Conclusion

In this article we have analyzed the bifurcation diagram of the Jaynes-Cummings model. The use of Lax pair techniques proved to be very useful. The classical analogue of algebraic Bethe Ansatz allows a very easy construction of the normal forms near critical points. We have shown in this way that this model possesses singularities of the elliptic and focus-focus type only. This is an approach alternative to the one due to Krichever [15] and based on the spectral curve. The spectral curve however was a very powerful tool to draw the full bifurcation diagram as advocated by Michèle Audin [8]. In the one spin case we get results in agreement with general considerations ([13, 18]), while in the two spins case it exhibits quite a rich structure which calls for more detailed investigations.

Along the open questions is the determination of normal forms along the lines of rank one, and the explicit construction of *real* solutions of the equations of motion along these lines. Another fascinating subject is the emergence of this classical geometry from the quantum system and Bethe equations [26]. We hope to return to these questions in future publications.

References

- [1] John Williamson, *On the Algebraic Problem Concerning the Normal Forms of Linear Dynamical Systems*. American Journal of Mathematics, Vol. 58 No. 1 (1936), pp. 141-163.
- [2] V. I. Arnold, *Mathematical Methods of Classical Mechanics*, Springer, New-York, 1997, Appendix 6.
- [3] L. H. Eliasson *Normal forms for Hamiltonian systems with Poisson commuting integrals - elliptic case* Comment. Math. Helvetici 65 (1990) pp. 4-35.
- [4] R. H. Dicke, *Coherence in spontaneous radiation processes*, Phys. Rev. **93**, 99 (1954).
- [5] E. Jaynes, F. Cummings, Proc. IEEE vol. 51 (1963) p. 89.
- [6] M. Gaudin, **La Fonction d' Onde de Bethe**. Masson, (1983).
- [7] E. Yuzbashyan, V. Kuznetsov, B. Altshuler, *Integrable dynamics of coupled Fermi-Bose condensates*. Phys. Rev. B **72** (2005), p. 144524.
- [8] M. Audin, *Spinning tops*, Cambridge University Press 1996.
- [9] M. F. Atiyah, *Convexity and commuting Hamiltonians*. Bull. London Math. Soc. 14(1) (1982) pp. 1-15.

- [10] V. Guillemin, S. Sternberg, *Convexity properties of the momentum mapping*. Invent. Math. 67(3) (1982) pp. 491-513.
- [11] San Vũ Ngoc *Moment polytopes for symplectic manifolds with monodromy*. Adv. Math. **208** (2007), pp. 909-934
- [12] H. Duistermaat, *On Global Action-Angle variables*, Comm. Pure Appl. Math. 33 (1980) pp. 687-706.
- [13] Alvaro Pelayo, San Vũ Ngoc. *Hamiltonian dynamics and spectral theory for spin-oscillators*. ArXiv 1005.0439.
- [14] O. Babelon, B. Douçot, L. Cantini, *A semiclassical study of the Jaynes-Cummings model*. J. Stat. Mech. (2009) P07011.
- [15] I. Krichever, *“Hessians” of integrals of the Korteweg-De Vries Equation and Perturbations of Finite-Zone Solutions*. Soviet Math. Dokl. Vol. 27 (1983), No. 3, pp. 757-761.
- [16] M. Audin, *Hamiltonian Monodromy via Picard-Lefschetz theory*. Comm. Math. Phys. 229 (2002) pp. 459-489.
- [17] M. Zou, *Monodromy in two degrees of freedom integrable systems*, J. Geom. Phys. **10**, (1992) p. 37.
- [18] N. T. Zung, *A note on focus-focus singularities*, Lett. Math. Phys. **60**, (2002), pp. 87-99.
- [19] N. T. Zung, *Another note on focus-focus singularities*, Diff. Geom. Appl. **7**, (1997), p. 123.
- [20] R. Cushman and J. J. Duistermat, *Non-Hamiltonian monodromy*, J. Diff. Eqs. **172**, (2001) p. 42.
- [21] B.A. Dubrovin, I.M. Krichever, S.P. Novikov, *Integrable Systems I*. Encyclopedia of Mathematical Sciences, Dynamical systems IV. Springer (1990) p.173–281.
- [22] O. Babelon, D. Bernard, M. Talon, **Introduction to Classical Integrable systems**. Cambridge University Press (2003).
- [23] O. Babelon, M. Talon, *Riemann surfaces, separation of variables and classical and quantum integrability*. Phys. Lett. A. 312 (2003), pp. 71-77.
- [24] E. Sklyanin, *Separation of variables in the Gaudin model*. J. Soviet Math., Vol. 47, (1979) pp. 2473-2488.
- [25] P. Griffiths and J. Harris, *Principles of algebraic geometry*, Wiley, New-York (1978), chapter 2.

- [26] O. Babelon, D. Talalaev, *On the Bethe Ansatz for the Jaynes-Cummings-Gaudin model*.
J. Stat. Mech. (2007) P06013.